frontiers | Frontiers in Chemical Engineering

TYPE Original Research
PUBLISHED 09 February 2024
DOI 10.3389/fceng.2024.1294752

OPEN ACCESS

EDITED BY
Ernesto Salzano,
University of Bologna, Italy

REVIEWED BY
David Alique Amor,
Rey Juan Carlos University, Spain
Amjad Riaz,
Yeungnam University, Republic of Korea
Gianmaria Pio,
University of Bologna, Italy
Eugenio Meloni,
University of Salerno, Italy

*CORRESPONDENCE
M. Van Sint Annaland,
m.v.sintannaland@tue.nl

RECEIVED 15 September 2023
ACCEPTED 02 January 2024
PUBLISHED 09 February 2024

CITATION
Pouw S, Bevers M, Gallucci F and Van Sint Annaland M (2024), A thermodynamic comparison of membrane-assisted processes for hydrogen production with integrated CO_2 capture.
Front. Chem. Eng. 6:1294752.
doi: 10.3389/fceng.2024.1294752

A thermodynamic comparison of membrane-assisted processes for hydrogen production with integrated CO_2 capture

S. Pouw[1], M. Bevers[1], F. Gallucci[2] and M. Van Sint Annaland[1]*

[1]Department of Chemical Engineering, Eindhoven University of Technology, Eindhoven, Netherlands, [2]Department of Chemical Engineering and Chemistry, Inorganic, Eindhoven University of Technology, Eindhoven, Netherlands

The energy efficiency of two novel process designs for the production of ultra-pure hydrogen with simultaneous capture of CO_2 using CH_4 as the feedstock, namely membrane-assisted chemical looping reforming (MA-CLR) and membrane-assisted sorption-enhanced reforming (MA-SER) has been compared. The modelling of the integrated network for mass and heat balances has been carried out using the ASPEN® Plus V10 process simulation tool to quantify the benefits and disadvantages of integrating hydrogen perm-selective membranes with either chemical looping or sorption-enhanced reforming. The evaluation of the MA-CLR process is carried out for a range of the following operating conditions: $10 < p_R < 60$ bar, $500 < T_R < 900$°C, and $1.5 < H_2O/CH_4 < 3.0$. On the other hand, for the MA-SER process the operation ranges of $1.0 < p_R < 10$ bar, $400 < T_R < 900$°C, and $2.5 < H_2O/CH_4 < 4.0$ were considered. Within the operation window of the MA-SER process, no carbon formation is observed, as any carbon present in the system reacts with CaO in the form of CO_2. However, in the case of the MA-CLR process, carbon formation can occur during the pre-reforming stage, particularly at low H_2O/CH_4 ratios. In terms of hydrogen yield, energy utilization and carbon capture, the MA-CLR outperforms the MA-SER plant. However, the MA-SER plant offers certain advantages over the MA-CLR system, such as a pure CO_2 product stream and lower reactor design temperatures. In the MA-CLR system, a carbon capture rate of 99.8% and a hydrogen product yield of 74.4% are achieved, whereas the MA-SER plant achieves a carbon capture rate of 98.5% and a hydrogen product yield of 69.7%.

KEYWORDS

hydrogen production, CCS/CCU, membrane assisted chemical looping reforming, membrane assisted sorption enhanced reforming, energy analysis

Introduction

The expected increase in global energy demand in the near future gives rise to major challenges from a geopolitical and technical point of view. It is projected that the demand for primary energy sources increases from 576.145 PJ/year in 2016 to 720.181 PJ/year in 2040 (ExxonMobil, 2018; IEA, 2018). In the first decades of the 21st century, the majority of this energy is generated from non-renewable resources such as oil, coal and natural gas, accounting for 32%, 27% and 22% respectively (IEA, 2018). However, the reliance on non-renewable sources contributes to greenhouse gas emissions. To ensure sustainable living conditions and limit the environmental impact, it is crucial to limit the global temperature

increase to 1.5°C compared to pre industrial levels (Masson-Delmotte et al., 2019). Achieving this goal requires significant reductions in CO_2 emissions, necessitating effective regulation of greenhouse gases. One approach taken by governmental institutions is the implementation of carbon taxes and emission rights to restrict total CO_2 emissions. In the EU, this is regulated by the so-called European Emission Trading System, EU-ETC. The price for CO_2 emissions under this system was around 4–7 €/ton in 2014, but has since risen to over 25 €/ton in Q1-2021 (Markets Insider, 2021). Projections indicate that the CO_2 price will continue to increase due to lower emission allowances in the coming decades, leading to higher operational costs (Marcu et al., 2016). Consequently, there is a growing demand for cost-effective CO_2 separation techniques to integrate into both existing and new plant designs.

Various technologies, collectively known as carbon capture and storage (CCS), have been developed to economically recover CO_2 from process streams (Metz et al., 2005; Cannone et al., 2021; Carpenter and Long, 2017). Three different process routes can be distinguished: post-combustion, pre-combustion and oxyfuel combustion. In this article, our focus will be on the utilization of pre-combustion and oxy-fuel combustion, with hydrogen as the primary product.

Hydrogen holds significant potential as a clean energy carrier and can contribute to achieving emissions targets. This is due to its high energy density ($\Delta H_c^0 = 120$ MJ/kg), and the fact that its combustion with oxygen from air results in steam, which has negligible environmental impact and is widely used as feedstock in numerous chemical processes. Currently, approximately 70 million tons of hydrogen are produced each year, with a market value of $103 billion USD in 2017. Projections indicate that the hydrogen market will experience an annual growth rate of 8.1% until 2026 (IEA, 2019; Research and Markets, 2019). However, the majority of hydrogen production still relies on fossil fuels. To transition towards sustainable practices with zero or even negative carbon footprints, there is a need for a transition period. This involves shifting away from non-renewable carbon-based energy sources while integrating carbon capture and storage (CCS) techniques. Simultaneously, the production of renewable energy carriers should be increased. This transitional phase is necessary until it becomes economically feasible to fully embrace sustainable chemical processes.

The following section describes the traditional methane steam reforming plant, which serves as a benchmark for large scale hydrogen production. The purpose is to identify the necessary improvements in material and energy efficiencies to enhance hydrogen production.

Industrial steam reforming of natural gas

Steam methane reforming (SMR) is the dominant method for large-scale hydrogen production and accounts for approximately 50% of the global hydrogen production (IEA, 2019; Ewan and Allen, 2005). Figure 1 provides a schematic representation of a traditional SMR plant which involves several steps, including feedstock pretreatment, reactor section, post-process treatment, and energy management. The process begins with the pretreatment of the natural gas (NG) feedstock, after which is undergoes reforming with steam in a reformer reactor. The first step consists of the pre-reforming of hydrocarbons to produce syngas through the steam reforming reaction (SR), shown in Eq 1, presented in Table 1. In the case of methane as the carbon feedstock ($n = 1$, $m = 4$), the steam methane reaction (SMR, Eq 2) yields a syngas with a stoichiometric ratio of 1: 3 for CO to H_2. This is followed by the water-gas shift reaction (WGS, Eq 3), which further increases the hydrogen yield but also generates CO_2. This process is thermodynamically limited and the enthalpies of formation indicate the SMR reaction is favored at elevated temperatures and low pressures, while the WGS is favored at low temperatures. To accommodate this suboptimal situation, the reformer reactor is operated at a high temperatures (700°C–1,100°C) and moderate pressures of 13–25 bar (Rostrup-nielsen and Rostrup-nielsen, 2002). This enables high methane conversion and results in

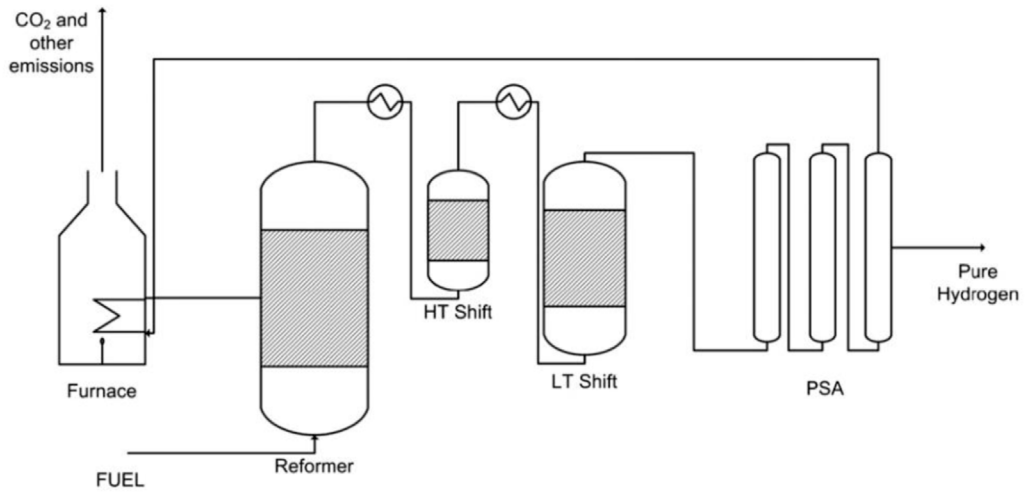

FIGURE 1
Benchmark SMR plant for hydrogen production using methane feedstock for the high temperature endothermic reaction in the reformer reactor. Direct combustion of methane with air leads to a low concentration CO_2 in the flue gas stream (Gallucci et al., 2013).

TABLE 1 Governing reactions for SMR plant.

Abr.	Reaction	$\Delta H^0_{r,298K}$ [kJ/mol$_{ref}$]	Ref. comp.	Eq
SR	$C_nH_m + nH_2O \rightarrow nCO + (n + \frac{m}{2})H_2$	+495.1	C_3H_8	(1)
SMR	$CH_4 + H_2O \leftrightarrow CO + 3H_2$	+206.0	CH_4	(2)
WGS	$CO + H_2O \leftrightarrow CO_2 + H_2$	−41.1	CO	(3)
MC	$CH_4 + 2O_2 \rightarrow CO_2 + 2H_2O$	−890.7	CH_4	(4)

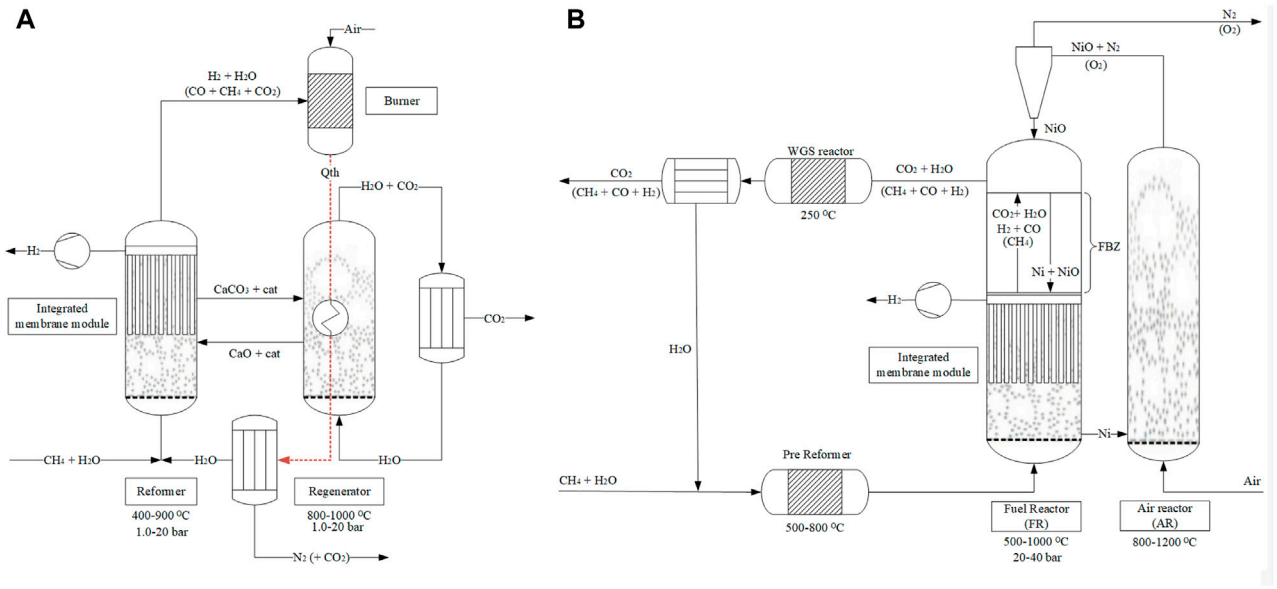

FIGURE 2
Simplified process flow diagram for the **(A)** MA-SER and **(B)** MA-CLR processes based on a dual fluidized bed reactor design.

a syngas composition primarily consisting of CO, H_2 and unconverted H_2O, and lower concentrations of CH_4 and CO_2. The hot gas steam is then cooled to around 200°C–350°C, which promotes the WGS reaction in the low temperature shift reactor for increased H_2 yield and CO_2 as byproduct. The resulting product steam mainly consists of H_2, CO_2, and excess H_2O. After condensing the excess steam, the product is purified using pressure swing adsorption (PSA) (Shi et al., 2018) or cryogenic distillation (Xu et al., 2014), where CO_2 is stripped from the hydrogen product. The overall energy demand and the high operating temperature of the reformer reactor contribute to the efficiency penalty of the process. The required heat is typically supplied by combusting part of the NG feedstock with air (MC, Eq 4), which reduces carbon efficiency and increases CO_2 production. As air is used to react in direct contact with NG, a dilute stream of CO_2 with a large N_2 content (typically 3%–15%) is produced (Metz et al., 2005). Separating CO_2 from the flue gas becomes increasingly costly as the concentration decreases, leading to higher operational- and capital expenditures (OPEX and CAPEX) and further reducing the carbon efficiency of the plant.

In order to develop a novel hydrogen production plant that utilizes NG as feedstock and effectively reduces the CO_2 emission costs (considered either as reduced carbon taxes or reduced energy penalties for the separation), the following criteria need to be met:

- Integrated heat management for the endothermic methane reforming reaction.
- Integrated carbon capture combined with reduction in carbon emission avoidance cost.
- Reduction of the number of unit operations for CAPEX and OPEX cost.
- Production of high-grade hydrogen (>99.99%) for fuel cell applications (Sasaki et al., 2019; Tawfik et al., 2007; Bacquart et al., 2019).

This study investigates two novel process designs that aim to achieve high-grade hydrogen production and integral CO_2 capture using methane as the feedstock. The first process is the membrane-assisted sorption-enhanced reforming (MA-SER), while the second process is the membrane-assisted chemical looping reforming (MA-CLR). Figures 2A, B provide a schematic representation of these processes. These processes achieve an effective physical separation of the reformate and the air stream, thereby removing the requirement for downstream N_2/CO_2 separation as is otherwise required in traditional processes. These processes achieve this in a different manner: the MA-SER process uses carbon transfer, whereas the MA-CLR process utilizes oxygen transfer. In literature the SER and CLR

process are investigated at various operation conditions using kinetic and thermodynamic models, including proof of demonstrations of the materials and reactor design. However, these processes are not yet evaluated in literature using a full heat- and mass integrated plant design with a sensitivity analysis. This work aims to provide insight on the advantages and disadvantages of the MA-SER and MA-CLR processes at plant design level. Both the MA-SER and MA-CLR processes rely on hydrogen perm-selective membranes and require further investigation into the current state-of-the-art H_2 membranes. Literature suggests that selectively removing reductive gasses from syngas streams *in situ* can enhance stable carbon formation on the catalyst (Oertel et al., 1987; Pedernera et al., 2007; Lægsgaard Jørgensen et al., 1995). To explore this phenomenon, a reference system known as membrane-assisted steam methane reforming (MA-SMR) is utilized, and the findings are extrapolated to inform the design and operation of the MA-SER and MA-CLR plant designs.

The subsequent sections provide a more detailed description of the MA-CLR and MA-SER processes. A preliminary thermodynamic study is performed to determine the optimal and stable process conditions for each process. Additionally, a comprehensive sensitivity study using a heat and mass balance (H&MB) integrated network is performed to assess the effects of operating conditions on the overall plant performance. To compare the two plant designs, key performance indicators (KPIs) are defined, presented on page 20. While this study primarily focuses on the technical aspects, a brief discussion on the economic aspects of the plant design will be provided, with a complete techno-economic analysis planned for future investigation.

MA-CLR process description

Figure 2B illustrates the configuration of the MA-CLR process, which is based on the chemical looping reforming (CLR) process. This process involves two interconnected fluidized bed reactors, the air reactor (AR) and the fuel reactor (FR). The solids circulation transfers the solids between the two reactors, while the gas streams remain physically separated (Fan, 2014; Rydén et al., 2006; Abad, 2015). The operation of this system relies on an oxygen carrier (OC), which is a solid compound responsible for transferring oxygen in the form of an oxidized (supported) metal from the air reactor to the fuel reactor. In the air reactor, the OC undergoes oxidation, generating heat and is increasing the temperature of the solids. This heat is utilized for the overall endothermic SMR and WGS reactions taking place in the fuel reactor. Various studies have been conducted to select an appropriate OC based on several criteria; such as thermal and mechanical stability, chemical activity for oxidation and reduction, multicycle performance, and cost considerations (Sub Kwak et al., 2018; Tang et al., 2015; Spallina et al., 2016; Kang et al., 2010). For this study, a Ni/NiO supported on γ-Al_2O_3 is chosen to investigate the MA-CLR process, serving as both the OC and catalyst for the SMR and WGS reactions. In the air reactor Ni is oxidized with the oxygen present in air to form NiO (OXOC, Eq 5), presented in Table 2. The (partially) oxidized and heated OC is then transferred to the fuel reactor, where it is reduced by the syngas mixture according to reactions in Eq 6-8. The solid particles are introduced at the top of the fuel reactor to reduce the reformate gas in the freeboard zone of the reactor. As a result, the gas stream leaving the FR primarily consists of CO_2 and H_2O, with traces of H_2, CO and CH_4. The (partially) reduced and moderately hot OC then re-enters the fluidized bed, acting as catalyst in its reduced state. To maintain autothermal conditions, the OC is removed from the fuel reactor and sent back to the air reactor, completing the chemical looping cycle of the OC. The MA-CLR process offers several advantages over the traditional SMR process:

TABLE 2 Governing REDOX reactions in MA-CLR process using methane as feedstock.

Abr.	Reaction	$\Delta H^0_{r,298K}$ [kJ/mol$_{ref}$]	Ref. comp.	Eq
Air Reactor				
OXOC	$2Ni + O_2 \rightarrow 2NiO$	−244.0	Ni	(5)
Fuel reactor				
REDOC 1	$NiO + CH_4 \rightarrow Ni + CO + 2H_2$	+204.0	NiO	(6)
REDOC 2	$NiO + CO \leftrightarrow Ni + CO_2$	−38.6	NiO	(7)
REDOC 3	$NiO + H_2 \rightarrow Ni + H_2O$	+2.5	NiO	(8)

- The oxidation of Ni in the air reactor generates the necessary energy for the endothermic SMR reaction in the fuel reactor. This eliminates the need for an external furnace, resulting in energy savings.
- The use of membranes in the MA-CLR process replaces the need for dedicated WGS reactors. By extracting hydrogen from the system, the thermodynamic equilibrium is shifted towards higher methane conversion, reducing the requirement for additional post-processing unit operations.
- In the MA-CLR process, oxygen is transferred through a solid matrix and used in the reforming reactions. As a result, the N_2 and CO_2 rich streams are physically separated without the need for additional separation equipment.

While the MA-CLR process employs an OC to transfer oxygen on a solid carrier to the FR for the reforming reactions, the MA-SER process on the other hand operates by cycling carbon in the solid matrix from the first to the secondary reactor before the fuel comes into contact with air. In the following section, we will provide a more detailed description of the MA-SER process.

MA-SER process description

A depiction of the configuration of the MA-SER process can be observed in Figure 2A. The framework of the MA-SER process is based on the sorption-enhanced reforming (SER) process. The SER

TABLE 3 Governing in (MA-)SER process using CaO based sorbents.

Abr.	Reaction	$\Delta H^0_{r,298K}$ [kJ/mol$_{ref}$]	Ref. comp.	Eq
CaC	$CaO + CO_2 \leftrightarrow CaCO_3$	−178.0	CaO	(9)
CaH	$CaO + H_2O \leftrightarrow Ca(OH)_2$	−104.2	CaO	(10)
HC	$2H_2 + O_2 \rightarrow 2H_2O$	−241.8	H_2	(11)

process combines the catalytic reforming of hydrocarbons with the *in situ* capture of CO_2 using a solid CO_2 acceptor, known as a sorbent, within a single reactor (Harrison, 2008; Arstad et al., 2012; García-Lario et al., 2015). The removal of CO_2 from the hydrogen rich stream by a gas-solid reaction enhances methane conversion according to the Le Chatelier's principle. This reversible reaction, referred to as carbonation (CaC, Eq 9) fixes CO_2 to the sorbent, while the calcination regenerates the sorbent. This reaction is presented in Table 3. The choice of sorbent for *in situ* CO_2 capture depends on various criteria, including reformer and regeneration temperature, pressure, gas composition, and reactor design. Generally, the sorbent must exhibit a high affinity for carbonation and calcination under the specified operating conditions, possess high chemical and mechanical stability, demonstrate a high sorption capacity and be produced at a relatively low cost. Numerous studies have addressed these aspects, particularly focusing on economically viable CCS process deployment (Harrison, 2008; Abanades et al., 2004; Yan et al., 2020; Shokrollahi Yancheshmeh et al., 2016; Boon et al., 2014; Feng et al., 2007; Moore, 1992; Nakagawa and Ohashi, 1999). In this study, a CaO-based sorbent supported by an inert Mayenite ($Ca_{11}Al_{14}O_{33}$) is selected due to its excellent multicycle stability, relatively high sorption capacity, low mechanical abrasion, and consistently high reaction rates. In the presence of syngas mixture containing excess steam, two reactions can occur with CaO as the sorbent. At low temperatures and high steam content, the hydration reaction is preferred (CaH, Eq 10), whereas in the presence of CO_2 the carbonation reaction (CaC, Eq 9) becomes more prominent due to the higher affinity for CO_2 compared to H_2O. These reactions are reversible and subject to thermodynamic limitations. The equilibrium curves for H_2O and CO_2 with CaO are illustrated in Figure 9A. However, considering only thermodynamic properties is insufficient for optimal reactor design, as the kinetics of both the sorbent and catalyst play crucial roles. Two kinetic regimes are defined for the sorbent (Shokrollahi Yancheshmeh et al., 2016; Li et al., 2016). At low sorbent conversion, the reaction rate is primarily governed by the fast surface reaction, which is independent of the sorbent conversion. As the $CaCO_3$ layer increases, the slow carbonate diffusion to the unreacted core of CaO becomes the rate-limiting step in the diffusion-limited regime, as the diffusion path increases with conversion. The transition between the fast- and slow-kinetics-dominating regimes is determined by the operating conditions and granulate design.

For the design of the plant, the SER process can be implemented using either a fixed bed reactor configuration with multiple beds operated in different modes or using a dual fluidized bed reactor (DFBR) configuration. In this study, the DFBR setup is chosen for several reasons. Firstly, it helps minimize the temperature gradient across the reactor, which in turn enhances the mechanical stability of the membranes. Additionally, it improves mass transfer between the gas phase and the membrane surface compared to the design of a multi-tube membrane fixed bed reactor.

In order to optimize the process design in terms of the KPIs, a sensitivity analysis is conducted to evaluate the impact of operating conditions. This analysis aims to identify a stable operating regime for all unit operations and optimize productivity in terms of feedstock and energy utilization. Initially, a preliminary study is carried out to establish a baseline for the sensitivity analysis. This study examines the effect of various operating conditions on hydrogen yield, carbon capture rate (CCR), and energy efficiency, after heat and power integration of the MA-SER plant. For both the MA-CLR and MA-SER plants the effectiveness of the plant modification/design heavily depends on the membrane performance.

State of the art H2 selective membranes and effect of *in situ* extraction on process stability

One of the options to extract hydrogen *in situ* is the deployment of perm-selective membranes. Significant advancements have been made in recent decades in terms of material performance, particularly regarding mechanical and chemical stability (Dittmar et al., 2013; Yukawa et al., 2014; Ockwig and Nenoff, 2007; Arratibel et al., 2018). It has been established that different types of membranes used for hydrogen separation have widely varying operating windows regarding gas composition, temperature and pressure, presented in Table 4 (Gallucci et al., 2013). Consequently, the performance of membranes can vary significantly in terms of product selectivity and permeability. When selecting membranes for the MA-SMR, MA-SER, or MA-CLR processes, the reactor design must also be taken into consideration. In the case of a (dual) fluidized bed operation mode, it is necessary to study the mechanical stability of the membrane concerning the impact of granulates on the membrane surface. Numerous experimental studies have been conducted under various operating conditions in fluidized beds to demonstrate the technical feasibility of implementing thin-film dense membranes and their stability over extended periods of time (Medrano et al., 2016). For this particular study, dense membranes are chosen, either on metallic or ceramic supports depending on the operating temperature, because of their high hydrogen perm-selectivity and their proven suitability for fluidized bed operation. It should be noted that a techno-economic analysis and a technical feasibility study should be conducted to evaluate the selection of materials for the dense membranes and their design, for their mechanical stability and activity. The selective removal of primarily H_2 from the reactor *in situ* has an impact on the balance between reductive and oxidative gasses, which can potentially lead to carbon formation. It is essential to conduct a preliminary study to evaluate the influence of this factor on the reactor design.

TABLE 4 Comparison of different membrane types for H_2 separation and process conditions.

Membrane type	Polymeric	Microporous ceramic	Porous carbon	Dense metallic	Proton conducting dense ceramic
Materials	Polymers: polymide, cellulose acetate, polysulone, etc.	Silica, alumina, zirconia, titania, zeolites, metal organic frameworks (MOF)	Carbon	Palladium alloys	Perovskites (mainly $SrCeO_{3-\delta}$, $BaCeO_{3-\delta}$)
Temperature (^{O}C)	<100	200–600	500–900	300–700	600–900
H_2 selectivity	Low	5–139	4–20	>1,000	>1,000
H_2 flux (10^{-3} mol $m^{-2}{\cdot}s^{-1}$) at ΔP = 1bar	Low	60–300	10–200	60–300	6–80
Transport mechanism	Solution-diffusion	Molecular sieving	Surface diffusion, molecular sieving	Solution-diffusion	Solution-diffusion
Stability issues	Swelling, compaction, mechanical strength	Stability in H_2O	Brittle, oxidizing	Phase transition (causes embrittlement)	Stability in CO_2
Poisoning issues	HCl, SO_x, CO	-	Strong adsorbing vapors, organics	H_2S,HCl,CO	H_2S
Cost	Low	Low	Low	Moderate	Low

Carbon formation in (membrane assisted-) steam methane reforming based processes

Extensive studies have been conducted in the literature on the reforming of various feedstocks such as natural gas, LPG, naphtha and (bio-)oil streams using steam and/or oxygen, particularly in relation to carbon formation (Gao et al., 2012; Rice and Delmotte, 2007; Annesini et al., 2007; Chhiti et al., 2013; Lugvishchuk et al., 2018). The formation of carbon can have detrimental effects on the process. It can cause redirection of gas flow, leading to increased mass transfer resistance caused by pore blockage, as well as increased heat transfer resistance, which in turn reduces the performance of the catalyst and increases conditions conducive to further carbon formation (Behnam and Dixon, 2017; Seemann and Thunman, 2019; Arku et al., 2020). During the reforming of hydrocarbons to syngas, carbon formation occurs as an intermediate step on the catalyst surface, and it is subsequently released from the surface in the form of CH_4, CO or CO_2. However, if the process conditions are not well optimized, amorphous carbon can cover the catalyst surface, resulting in reduced catalytic activity due to fewer available catalytic sites. Eventually, the entire surface becomes covered in carbon, leading to catalyst deactivation. To prevent stable carbon formation, extensive thermodynamic studies have been carried out. These studies consider the effects of steam-to-carbon (H_2O/CH_4) and oxygen-to-carbon ratios, as well as temperature and pressure. Surface models, such as molecular dynamics, take into account the orientation of catalyst crystals and their interaction with the support surface, as macro thermodynamic parameters alone do not capture the changes in entropy and adsorption enthalpy occurring at the catalyst surface. These surface models help elucidate the impact of these microscopic factors on carbon formation and can lead to a shift in the regime of stable carbon formation at higher H_2O/CH_4 ratios, which may differ from what is predicted by macro thermodynamic properties (Jaworski et al., 2017).

TABLE 5 Governing reactions carbon formation from methane feedstock.

Abr.	Reaction	$\Delta H^0_{R,298K}$ [kJ/mol_{ref}]	Ref. comp	Eq
MD	$CH_4 \leftrightarrow C(s) + 2H_2$	+74.9	CH_4	(12)
rB	$2CO \leftrightarrow C(s) + CO_2$	−172.5	CO	(13)

When using CH_4 as feedstock, these reactions involved are classified as the methane decomposition (MD, Eq 12) and the reverse Boudouard (rB, Eq 13) reaction, as shown in Table 5. The MD reaction is favored at low pressures and high temperatures, whereas the rB reaction is favored at high pressures and low temperatures. This interplay between temperature and pressure is relevant because it influences the source of stable carbon formation, indicating that suboptimal condition can lead to undesired production of carbon.

In the respective sections of the MA-CLR and MA-SER processes, the impact of process conditions on carbon formation is investigated, with the MA-SMR process serving as benchmark for comparison. To assess and compare the performances of plants, it is necessary to establish a methodology for designing the plants. This methodology will outline the criteria and considerations used in designing the MA-CLR and MA-SER processes, allowing for a comprehensive evaluation of their performances and facilitating a meaningful comparison with the benchmark MA-SMR process.

Process simulation methodology

The calculation of the integrated network of mass and heat balances is carried out using the ASPEN® Plus V10 simulation tool. This software tool enables the incorporation of physical properties and chemical interactions of compounds under varying operating conditions. It allows for the combination of different unit

TABLE 6 MA-CLR and MA-SER operation conditions and material composition.

MA-CLR		
Oxygen carrier: Ni, $MgAl_2O_4$ (Medrano et al., 2017)	[wt%]	20, 80
Retentate pressure	[bar]	10–60
Permeate pressure	[bar]	1.0–5.0
H_2O/CH_4 inlet	[mol/mol]	1.5–3.0
Fuel reactor temperature	[°C]	400–900
H_2 selectivity	[-]	Infinite
Partial pressure difference membrane H_2	[bar]	0.2
Oxygen excess inlet	$[mol_{O2}/mol_{O2,stoic}]$	1.2
MA-SER		
Sorbent: CaO, Mayenite	[wt%]	30, 70
Catalyst: Ni, $MgAl_2O_4$ (Martínez et al., 2013)	[wt%]	15, 85
Retentate pressure	[bar]	1.0–10
Permeate pressure	[bar]	Variable
H_2O REG pressure	[bar]	$\max(p_{ret}, 5.0)$
H_2O/CH_4 inlet	[mol/mol]	2.5–4.0
Sorbent/catalyst	[kg/kg]	3.0
CaO/CH_4	[mol/mol]	1.0–3.0
Reformer reactor temperature	[°C]	400–900
H_2 selectivity	[-]	Infinite
Partial pressure difference membrane H_2	[bar]	0.1
Oxygen excess inlet	$[mol_{O2}/mol_{O2,stoic}]$	1.2

operations, such as mixers, splitters, reactors, heat exchangers, (multistage) compressors, expanders, to design a chemical plant. For example, the membrane fluidized bed reactor is not a standard unit operation but can be constructed and simulated by first combining the solid inlet stream from the top of the reactor and the reforming feedstock mixture. The gas-solid mixture is converted such to maximize the hydrogen content in a RConv reactor. Based on the H&MB network a fraction of the hydrogen is removed using a FSplit operator and finally the remaining gas-solid mixture is obtained at equilibrium composition by a RGibbs reactor. Another example is this the freeboard zone of the FR where the solid and gas streams flow countercurrent. This is simulated using three combinations of a single RGibbs reactor and a FSplit operator. The downward solid flow and upward gas flow are combined as inlet to the RGibbs reactor to obtain an equilibrium composition. The oulet of this RGibbs reactor is separated using a FSplit operator such that the solid flow is either send to reactor N-1 or to the FR. For the gasflow this is send either as inlet to RGibbs reactor N+1 or to the heat exchanger of the pre-reformer.

To simplify the system and limit the number of variables, several design specifications and calculators are implemented to ensure operation within the desired conditions. Table 6 provides an overview of the material composition and operating conditions used in this study. The heat integration is based on pinch analysis, which involves utilizing heat exchange between high-temperature streams that need to be cooled and low-temperature streams that need to be heated, in order to minimize the heat exchange equipment size and maximize the recovery of high caloric energy in the system (El-Halwagi, 2006).

Performance indicators for MA-SER and MA-CLR process design

In the comparison between the H&MB integrated MA-SER and MA-CLR plants, which are operated at different optimal process operation conditions, various performance indicators are defined to assess both feedstock- and energy utilization.

Table 7 provides an overview of the performance indicators used in this study and Table 8 provides the base assumptions for modelling of process schemes of the MA-CLR and MA-SER process. Both the MA-SER and MA-CLR processes utilize CH_4 as carbon feedstock. For the reforming plants, three product streams are defined: (1) the hydrogen extracted from the reformate using perm-selective membranes, (2) the CO_2-rich stream and (3) the high-temperature depleted air stream. The primary objectives of both processes are: (1) maximize the hydrogen yield, (2) minimize CO_2 emissions, considering the energy penalty associated with separation and (3) achieve optimal energy recovery through a heat-and-power integrated network.

The assessment of hydrogen production in the MA-SER and MA-CLR processes involves monitoring two key performance indicators: the hydrogen recovery factor (HRF, Eq 14) and the hydrogen yield (Y_{H2}, Eq 15). The hydrogen recovery factor (HRF) is calculated as the ratio of the hydrogen permeation rate to the maximum hydrogen production rate achievable from the hydrocarbon feedstock when using H_2O as an oxidizer. This factor provides an indication of how effectively hydrogen is recovered from the system. The hydrogen yield (Y_{H2}) represents the amount of hydrogen produced relative to the maximum hydrogen production rate from the hydrocarbon feedstock using H_2O as an oxidizer. It accounts for the hydrogen permeation rate and the product stream, providing a measure of the efficiency of hydrogen production. In addition to hydrogen production, reducing carbon emissions is a crucial aspect of the MA-SER and MA-CLR processes, which is monitored with the carbon capture rate (CCR, Eq 16), defined as the carbon molar flow rate in the form of CO_2 captured compared to the total carbon molar feedstock flow rate, in compliance with purity constrains specified in EU regulations for geological storage (Anantharaman et al., 2011).

To assess the overall energy efficiency of the process, two energy-based performance indicators are defined. The first indicator is the hydrogen efficiency (η_{H2}, Eq 18), which represents the chemical energy stored in the hydrogen product from CH_4, not considering other forms of energy. The second indicator is the equivalent hydrogen efficiency (η^{ev}_{H2}, Eq 19), which evaluates the overall energy conversion efficiency of the hydrogen plant. This indicator takes into account the recoverable thermal energy which can be used for auxiliaries or steam transport and the

TABLE 7 Performance indicator for hydrogen plant comparison (Martínez et al., 2013).

Performance indicator	Description	Equation	Unit	Eq
HRF	Hydrogen recovery factor	$HRF = \frac{F_{H2}^{perm}}{4 \cdot F_{CH4}^{0}}$	–	(14)
Y_{H2}	Hydrogen Yield	$Y_{H2} = \frac{F_{H2}^{prd}}{4 \cdot F_{CH4}^{0}}$	–	(15)
CCR	Carbon capture rate	$CCR = \frac{y_{CO2}^{prd} F_{CO2}^{prd}}{F_{CH4}^{0} + F_{CO2}^{0}}$	–	(16)
CCR^{ev}	Equivalent carbon capture rate	$CCR^{ev} = \frac{y_{CO2}^{prd} F_{CO2}^{prd} + \frac{Q_{th}}{E_{th}^{ref}} + \frac{W_{el}}{E_{el}^{ref}}}{F_{CH4}^{0} + F_{CO2}^{0}}$	–	(17)
η_{H2}	Hydrogen efficiency	$\eta_{H2} = \frac{LHV_{H2} \cdot F_{H2}^{prd}}{LHV_{CH4} \cdot F_{CH4}^{0}}$	–	(18)
η_{H2}^{ev}	Equivalent hydrogen energy efficiency	$\eta_{H2}^{ev} = \frac{LHV_{H2} \cdot F_{H2}^{prd} + Q_{Th} \eta_{Th}}{LHV_{CH4} \cdot F_{CH4}^{0} + \frac{W_{el}}{\eta_{el}}}$	–	(19)
E_{CO2}	CO_2 specific emission avoidance cost	$E_{CO2} = \frac{y_{CO2}^{prd} F_{CO2}^{prd}}{F_{H2}^{prd} \cdot LHV_{H2}}$	$\frac{kg_{CO2}}{GJ}$	(20)
E_{CO2}^{ev}	Equivalent CO2 specific emission	$E_{CO2}^{ev} = \frac{y_{CO2}^{prd} F_{CO2}^{prd} + Q_{th} E_{th}^{ref} + W_{el} E_{el}^{ref}}{F_{H2}^{prd} \cdot LHV_{H2}}$	$\frac{kg_{CO2}}{GJ}$	(21)
f_{el}^{imp}	Fraction electricity import to methane feedstock	$f_{el}^{imp} = \frac{W_{el}}{W_{el} + LHV_{CH4} \cdot F_{CH4}^{0}}$	–	(22)
f_{Qth}^{exp}	Fraction steam export to hydrogen production	$f_{Qth}^{exp} = \frac{Q_{th}}{Q_{th} + LHV_{H2} \cdot F_{H2}^{prd}}$	–	(23)

overall electricity demand for compressors/expanders. These energy demand/production from auxiliaries must be corrected by their energy conversion efficiencies, which is typically $\eta_{th} = 0.90$ and $\eta_{el} = 0.583$ (Martínez et al., 2013).

The most important parameters to be monitored for a hydrogen plant using carbon feedstocks, based on thermodynamic studies, are the hydrogen efficiency and the CCR factor to produce the maximum amount of hydrogen, without compromising the energy cost associated with CO_2 separation from process streams. Therefore, in order to compare the conversion of different hydrogen plants using different carbon containing feedstocks and process conditions, the CO_2 specific emission avoidance cost (E_{CO2}, Eq 20) compares the energy stored in hydrogen with the amount of CO_2 which is not emitted. It takes into account the CO_2 emissions associated with the energy demand/export for auxiliaries. The equivalent CO_2 specific emission avoidance cost (E_{CO2}^{ev} , Eq 21) is a more accurate representation of the energy penalty for carbon capture. Finally, to assess the extent of the external energy infrastructure required for these processes, the import in the form of electricity or energy export in the form of steam compared to the chemical feedstock or products, are expressed in the electrical energy import (f_{el}^{imp}, eq 22) and thermal export fraction (f_{Qth}^{exp}, eq, 23). A lower import or export fraction indicates that the plant is less dependent on plant location, being more self-sufficient for energy production and utilization.

Carbon formation in membrane-assisted reforming processes

The study is performed in ASPEN® Plus V10 by the combination of a conversion reactor, a separator at a selected hydrogen recovery factor (HRF, Eq 14) and the remaining gas mixture is sent to a Gibbs equilibrium reactor. The outlet composition is determined by the Gibbs reactor, which minimizes the chemical potential energy where solid carbon is allowed as component to be formed next to CO, CO_2, CH_4, H_2O and H_2. In Figures 3A, B the impact of reforming pressure and a range of HRFs on the carbon formation regime is shown as a function of reforming temperature and inlet H_2O/CH_4 ratios. The lines indicate where the transition exist between the macroscopic favorable conditions for carbon formation on the left side, as more reductive gasses are present compared to the right side where no carbon deposition is expected due to the excess of oxidative gasses. Using $p_R = 5.0$ bara, HRF = 0 and $T_R = 650°C$ as example at $H_2O/CH_4 = 1.0$ stable carbon formation can be expected whereas at $H_2O/CH_4 = 2.0$ not. The model results are verified with literature for HRF = 0 (Annesini et al., 2007).

Prior to this study, there is limited literature available on the investigation of how hydrogen removal affects the shift of the stable carbon formation regime. Therefore, we aim to explore this aspect in the context of membrane-assisted reforming processes, with MA-SMR serving as the benchmark. By conducting this investigation, we intend to provide valuable insights into the impact of hydrogen removal on carbon formation. The MA-SMR process is schematically represented in Figure 4 where a fraction of the permeated hydrogen is used as fuel for the endothermic SMR reaction.

From the results, graphically presented in Figure 3, it can be observed that an increase in HRF has a significant effect on the position of the stable carbon formation regime. As hydrogen is removed, the production of CO and CO_2 through SMR and WGS is not desirable from a thermodynamic point of view. At lower temperatures methane is the most thermodynamically stable product. With increased methane concentrations the MD reaction is more beneficial to provide the desired hydrogen for extraction, shifting the carbon formation regime. At higher temperatures the formation of CO is the most thermodynamically stable product, resulting in a gradual

TABLE 8 Base assumptions for modelling of process schemes of MA-CLR and MA-SER process in ASPEN for M&HB integrated network for hydrogen production (Anantharaman et al., 2011; Spallina et al., 2016; Martínez et al., 2013; Turton et al., 2001).

Feedstock/product properties						
Stream	Type [-]	Composition [V/V %]	Pressure [bar]	Temperatue [°C]	LHV [kJ/mol]	Reference [-]
CH_4	Feedstock	100 (CH_4)	75	15	50	
CO_2	Product	≤ 0.2 (CO) ≤ 5.0 (H2 + CH4)	110	30	Variable	(Anantharaman et al., 2011; Martínez et al., 2013)
H_2	Product	100 (H_2)	150	30	120	
H_2O	Feedstock	100 (H_2O)	1.0	15	-	
Air	Feedstock	77.3, 20.74, 1.01, 0.92, 0.03 (N_2, O_2, H_2O, Ar, CO_2)	1.0	15	-	Anantharaman et al. (2011)

Energy export/import conversion efficiencies			Turton et al. (2001)
η_{th}	0.90	–	
η_{el}	0.583	–	
Pump/blower efficiencies			Turton et al. (2001)
η_{hydr}	0.80	–	
η_{mech}	0.94	–	
Compressor/expander efficiencies			Spallina et al. (2016)
η_{iso}	0.925	–	
η_{mech}	0.98	–	
CO_2 emissions associated per energy source			Turton et al. (2001)
$E^{ev}_{th,CO2}$	$63.3 \cdot 10^{-3}$	$\frac{kg_{CO2}}{MJ_{th}}$	
$E^{ev}_{el,CO2}$	$97.7 \cdot 10^{-3}$	$\frac{kg_{CO2}}{MJ_{el}}$	
E^{ev}_{CH4}	$55.0 \cdot 10^{-3}$	$\frac{kg_{CO2}}{MJ_{c}}$	
Minimum temperature difference in heat exchangers			Spallina et al. (2016)
ΔT_{gg}	20	°C	
ΔT_{gl}	10	°C	
T_{steam}	≥ 250	°C	
Steam export (LP)			Turton et al. (2001)
Temperature	200	°C	
Pressure	6.0	bar	

10.3389/fceng.2024.1294752

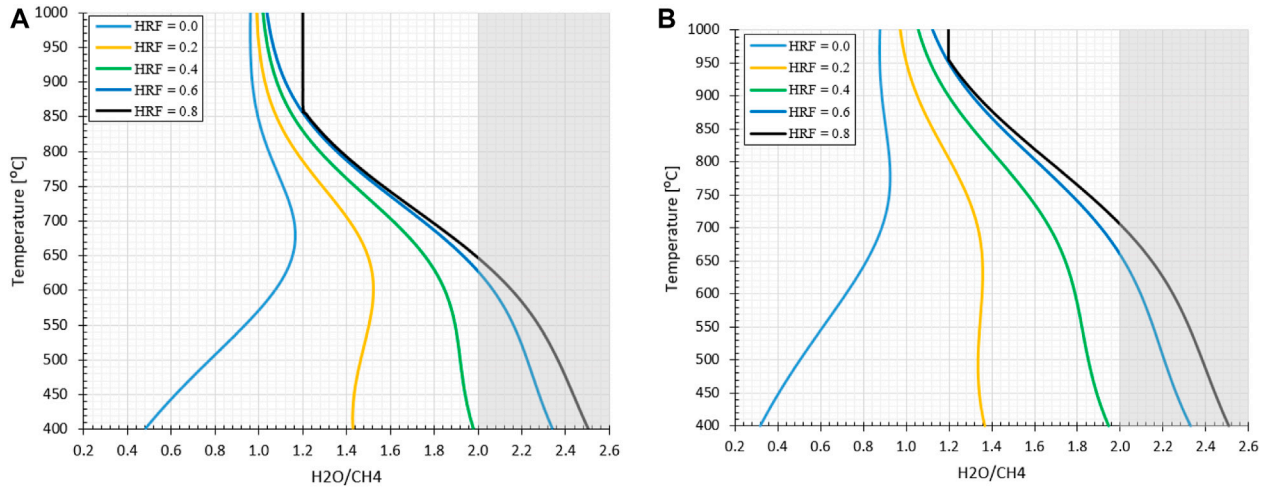

FIGURE 3
Effect of stable carbon formation regime as function of pressure and HRF for MA-SMR system **(A)** 5.0 bara **(B)** 20 bara. The gray shadow represents the conditions where the stoichiometric ratio is greater than 2.0, the minimal ratio required for full conversion of CH_4 to CO_2. The asymptote at HRF = 0.8 at elevated temperatures observed for H_2O/CH_4 at 1.2 is due to the competition between the production of H_2 for extraction through the SMR reaction and the undesirable conditions for WGS equilibrium.

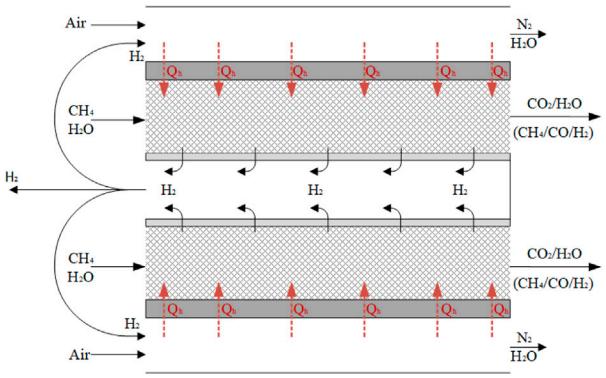

FIGURE 4
Schematic representation of MA-SMR reactor module. From inside to outside the H_2 perm selective membranes, the catalytic fixed bed, the heat exchanger wall and the combustion zone. The endothermic reaction for steam methane reforming is sustained by the combustion of H_2 with air, effectively separating CO_2 from N_2 stream while obtaining autothermal conditions.

transition between MD and rB dominating mechanism for carbon formation. This transition is observed in the curvature at intermediately high temperatures because of the presence of CO_2 as intermediate stable product in steam reforming, generating a transition zone. In this section with increasing temperature the MD and SMR are more favorable, where the conversion of CO from the rB reaction is prevented by the CO_2 presence in the syngas mixture. In conclusion, It can be observed that the trade-off between the MD, which is favorable at low temperatures and lower pressures and the rB, favorable at high temperatures and pressures, results in a gradual transition of the stable carbon formation boundary indicated with the lines. This is with respect to both increasing pressures and temperatures due the interplay in most favorable conditions/enthalpy and net gaseous products.

A final important note is the potential for carbon formation in the MA-SMR at relatively low HRF values, exceeding the stoichiometric ratio of 2.0 for full CH_4 conversion to maximize Y_{H2}. To prevent this phenomenon, excess of steam is required throughout each position in the reactor. This is also beneficial from a thermodynamic point of view, increasing the driving force for the SMR and WGS reactions. However, from an economic point of view, this increases the plant size and results in larger heat sinks for the condensation and reheating of the vapor stream which reduces the overall energy efficiency of the plant. In membrane reactors the excess steam reduces the hydrogen partial pressure and results in a lower driving force across the membrane. In order to compensate for this reduction additional membrane area and/or lower permeate pressure, e.g. lower pressure or increased sweep flow rate, is required to recover the hydrogen product. This induces an increase in OPEX and CAPEX cost with increasing H_2O/CH_4 ratios.

In the next sections for individually the MA-CLR and MA-SER process a preliminary thermodynamic analysis is performed to 1) establish the optimal process conditions 2) investigate the effect of process conditions using a sensitivity analysis in an H&MB integrated system on the KPIs.

Thermodynamic preliminary analysis for MA-CLR process

In order to operate the (MA-)CLR process at autothermal operation conditions the ideal H_2O/CH_4 and oxygen-to-methane (O_2/CH_4) ratio is determined by balancing the exothermic energy from the methane oxidation and WGS with the endothermic SMR reaction using Hess law. This can be achieved by combining reactions equations 09-11, from which the maximum hydrogen yield at autothermal conditions can be calculated. The ideal H_2O/CH_4 and O_2/CH_4 ratio are approximately 1.258 and 0.371

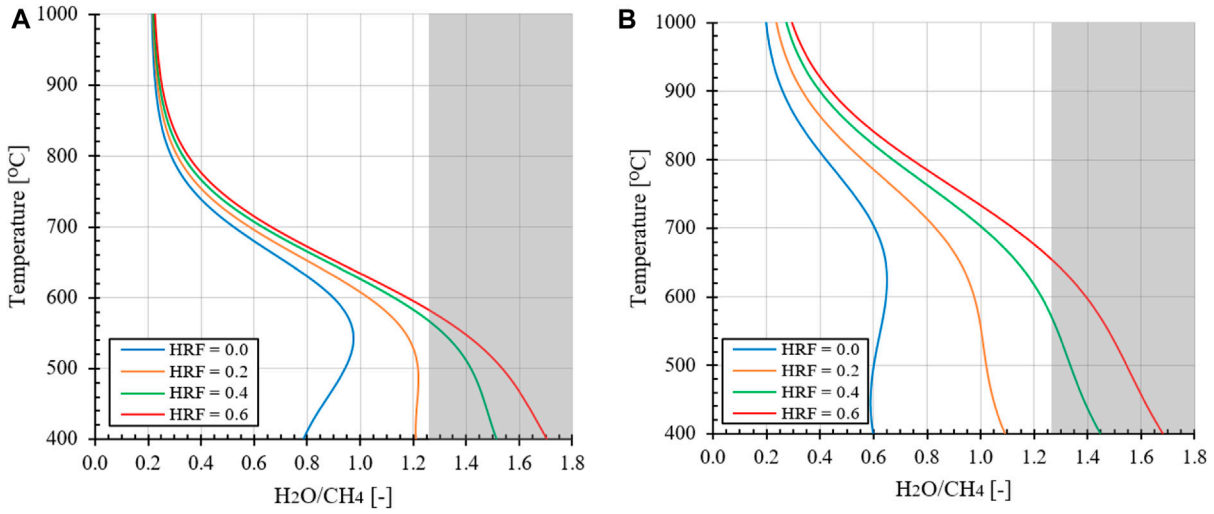

FIGURE 5
Effect of hydrogen extraction on stable carbon formation regime with O_2/CH_4 = 0.371 at **(A)** 1.0 bara and **(B)** 10 bara at variable reforming temperatures. The shaded area represents the H_2O/CH_4 ≥1.26 ratio required for autothermal operation conditions and minimum steam content for full conversion of the methane feedstock.

respectively for a wide temperature range between 400°C and 1,000°C. This corresponds with a $Y_{H2,max}$ = 0.897 at ideal autothermal conditions. To satisfy the overall energy demand due to dilution of oxygen in air and the overall energy demand of the system the simulations are performed for $CH_4/H_2O \geq 1.5$, while the O_2/CH_4 ratios are varied, taking into account an excess of 20% in the air reactor. As carbon formation is more prone at low O_2/CH_4 and H_2O/CH_4 ratios, this will be used as reference case for this study, for an isothermal system the O_2/CH_4 = 0.371 and is evaluated at different HRFs. A sensitivity study on carbon formation is performed to study the effect of HRF.

In Figure 5 the effect of hydrogen extraction with respect to the FR temperature is presented for an operation pressure at 1.0 or 10 bara. It can be observed that at higher HRFs the carbon formation regimes shifts from low to higher H_2O/CH_4 ratios, as expected from the analysis preformed for the MA-SMR system. It can be assumed that the oxygen from steam is partially substituted by molecular oxygen from air, which is fully consumed. It must be noted that at a moderate HRF ≥0.4 the ideal H_2O/CH_4 ratio based on autothermal operation conditions for low reforming temperatures raises concerns. This implies that an excess of steam is required for the operation of the MA-CLR system to ensure avoiding carbon formation at any position in the FR. For the evaluation of the MA-CLR system the overall process scheme is analyzed, which determines the minimum H_2O/CH_4 ratio required to prevent carbon formation.

Due to the design of the MA-CLR reactor the solids from the AR will first get into contact with the gas outlet from the fluidized bed section of the FR, partially reducing the OC. Therefor the local oxygen content entry from the top in the fluidized bed membrane reactor can be lower as more reductive gasses passes through the top of the reactor. The OC has two objectives: in the first place it is to supply the fuel reactor with sensible heat required for the endothermic reforming reactions, the secondary goal is to introduce atomic oxygen to the reactor to reduce the oxygen required from the steam. However, this can cause an imbalance in the local reactor gas and solid composition to prevent carbon formation. When the solids temperature is too low, the solid circulation rate is increased and more oxygen in the form of NiO is introduced in the fuel reactor; the reformer gasses are fully reduced at the end of the freeboard-zone. When the solid temperature from the air reactor is too high due to the efficient recovery of heat from the depleted air stream to the air feed, the solids circulation rate is reduced. Therefor the oxygen content in the OC introduced in the freeboard-zone is (fully) depleted by the reformer gasses from the fuel reactor before entering the fluidized bed section with membranes. This condition will lead effectively to a lower O_2/CH_4 ratio with a higher propensity to carbon formation. Considering these factors both from the thermodynamic sensitivity analysis and process design, a minimum H_2O/CH_4 ratio of 2.0 will be selected as lower boundary for the MA-CLR system in this investigation. Based on literature references the remaining base case process conditions are selected to be 600°C, p_{Ret} = 20 bar and p_{Perm} = 1.0 bar (Medrano et al., 2014).

The MA-CLR process is modelled in ASPEN® Plus V10 using the combination of the standard operation units available in the software package. The H&MB integrated MA-CLR process is presented in Figure 6. The integration network proposed is based on the preliminary analysis of the temperature profiles and energy demand of the unit operations and heat exchangers using pinch analysis. In order to simulate the plant, a set of constraints have to be implemented, in the form of design specs, to reduce the number of free variables in the system which are related to the heat and mass balances. These following design specs have been implemented in the ASPEN flowsheet, presented in Table 9:

1. In order to operate the fluidized bed section of the fuel reactor, where the membranes are located, the desired temperature is set as FR temperature. This temperature is the result of an

10.3389/fceng.2024.1294752

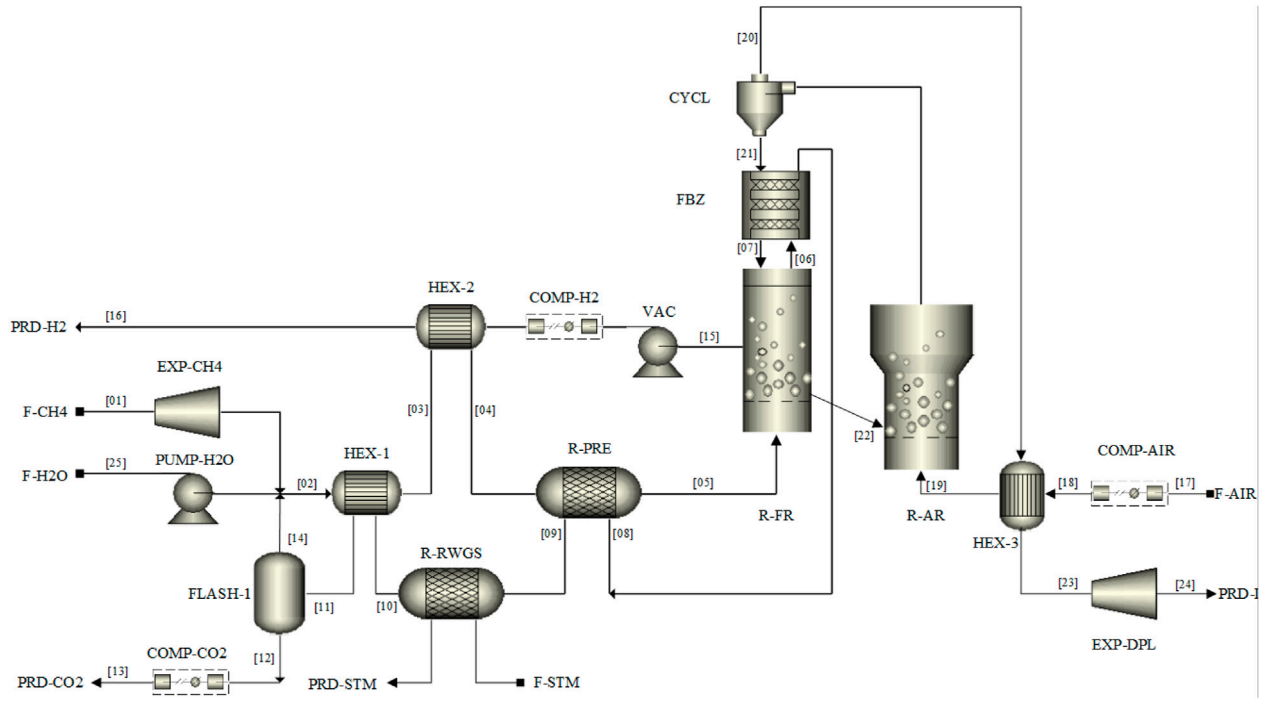

FIGURE 6
M&HB integrated network for MA-CLR hydrogen plant using DFBR configuration for continuous operation.

TABLE 9 Design specs for MA-CLR process.

Design spec	Formula	Variable parameter
Fuel reactor temperature	$\frac{-\sum Q_{in}}{\sum Q_{out}}\|_{FR} - 1 = 0$	OC circulation rate
Oxygen-to-OC ratio	$\frac{0.6*F_{O2}}{F_{Ni}}\|_{AR} - 1 = 0$	F-AIR
Inlet H_2O/CH_4 ratio	$\frac{F_{H2O}}{F_{CH4}}\|_{pre} - \text{Target} = 0$	F-H2O
Driving force membrane	$\frac{P_{Ret} y_{H2,Ret}}{0.2 p_{perm}} - 1 = 0$	HRF
Energy demand for pre-reforming	$\frac{T_{flue}^{out} - T_{R,pre}}{20} - 1 = 0$	TR pre

integral heat and mass balance which has to be solved by the combination of the heat of reaction due to the governing reactions, the temperature of the OC from the freeboard zone of the FR and the inlet of the reformate feedstock from the pre-reformer reactor. To obtain the design temperature, the solids circulation rate is adapted between the FR and AR.

2. To ensure that the reduced OC from the FR is fully oxidized an excess of oxygen in the AR is required. This excess is set at 20% compared to the stoichiometric amount for the oxidation reaction. Thus, the air feedstock flow rate is varied to achieve this required excess.
3. The inlet H_2O/CH_4 ratio for the pre-reforming reactor is a stream consisting of fresh H_2O feed and the recycle obtained from steam condensation after separation from the CO_2-rich stream from the flue gas. This is the result of the reduction of fuel with OC in the freeboard-zone and excess steam in the feed to the FR. Depending on the recycle stream flow rate, the fresh H_2O feed rate is adjusted.
4. In the case of integration with membranes, a driving force is required to extract the hydrogen *in situ* from the reformate stream in the FR. In order to maintain a significant driving force throughout the reactor the hydrogen outlet composition is controlled by the HRF such that the difference between the hydrogen partial pressure at the outlet of the REF reactor and the permeate pressure is 0.2 bar.
5. In order to improve the energy integration of the plant, the high-temperature flue gas stream from the FR can be utilized to supply the energy demand for the highly endothermic reforming reactions in the pre-reformer reactor. To supply the heat for the pre-reforming reactions a temperature difference is required between the streams. An energy balance is used where the temperature of the pre-reformer is varied such that the outlet flue gas temperature is 20°C above the outlet temperature of the reactor.

In Supplementary Appendix SA the composition, temperature and pressure of the individual streams, indicated by the stream

number in Figure 6, are presented for the basecase of the MA-CLR process of this study.

Sensitivity analysis MA-CLR plant for hydrogen production

It has been identified in the preliminary thermodynamic study that the effect of temperature, retentate pressure and oxygen content in the reactor has a significant influence on the stability of the MA-CLR process and the plant KPIs. Therefore, a sensitivity analysis using the base case parameters for the MA-CLR process is carried out. The retentate pressure is a free variable which can be changed independently. The fuel temperature is varied through the solids circulation rate, and the oxygen content in the fuel reactor is controlled by the permeate pressure.

The fuel reactor temperature has a significant impact on the stability and performance of the MA-CLR plant. Based on the preliminary analysis, it is anticipated that higher HRFs at lower FR temperatures may lead to a higher potential for carbon formation. This is indeed confirmed after heat and mass integration, as can be observed in Figure 7A. Fuel reactor temperatures above 550°C have minimal effect on the CCR and Y_{H2}, indicated by the slight negative slope in the plot, as the heat recovered at higher temperatures is used to facilitate the energy demand in other sections in the system. For the high temperature fuel off gas stream, this high heating value energy is used in the pre-reformer section to supply the energy required for the overall endothermic reactions. The high temperature from the depleted air stream generated in the AR, is used to heat the air feed for the oxidation of the OC in the AR. It must be noted that only heat integration is insufficient to consider the system performance. Increasing the FR temperature results in an increase in the AR temperature as the OC is supplying the oxygen and energy required for the endothermic reaction in the FR, as can be seen in Figure 7B. Another consideration is the CO content in the CO_2-rich offgas. Due to the higher temperatures in the freeboard-zone during reduction of the OC and the high CO_2 content, from a thermodynamic perspective it is undesirable to convert CO into CO_2 at elevated temperatures. This reduces the oxygen content in the offgas to the WGS reactor. Therefor a higher CO content is found in the CO_2 stream, which does not satisfy the quality requirements for geological storage applications when operating the FR at higher temperatures at 20 bar.

From a thermodynamic point-of-view, the retentate pressure is a minor impact on the hydrogen yield and the CCR, as shown in Figure 7C. This is explained by the fact that the reactions which involve the reduction of the oxygen carrier in FR or the oxidation in the AR are reactions that are not dominated by the effect of thermodynamic equilibrium shifts due to the full conversion of the reactants. In order to pressurize the system, multiple expanders and compressors have to be installed to operate at the desired retentate pressure for both the FR and AR. However, this compression energy is recovered for the depleted air stream and from the other product streams, viz. H_2 and CO_2-rich flue gas streams. This process step is already required as the product delivery pressure is higher than the reactor pressure. It must be noted that even though the reduction of the OC is independent of pressure the CO content in the flue gas is affected by the amount of H_2 at the outlet of the FR. Due to a lower H_2 content less OC is reduced in the freeboard zone, affecting the equilibrium of the catalytic SMR and WGS reactions at higher temperatures. These conditions result in an increase of CO in the offgas mixture.

The permeate pressure is a free variable which effectively regulates the amount of reductive gasses available for the reduction of the OC in the freeboard-zone. The permeate pressure is varied between 1.0 and 5.0 bara, as presented in Figures 7E, F. At low permeate pressure, more H_2 is recovered in the fuel reactor due to the higher membrane chemical potential difference between retentate and permeate side. This results in less H_2 leaving the fuel reactor section at the top of the fluidized bed section for the reduction of the OC in the freeboard-zone. As the heat demand in the fuel reactor is regulated by the OC circulation rate, a fixed amount of oxidized OC is sent to the freeboard-zone for reduction. If the amount of reductive gasses from the fuel reactor is limited by the process conditions, only a fraction of the OC is reduced and the remaining oxidized OC will enter the fluidized bed section. This effectively increases the oxygen content in the fuel reactor for the partial oxidation of methane. As the permeate pressure increases more H_2 is available for the reduction of the OC in the freeboard-zone, thereby lowering the effective oxygen content in the FR. This generates an environment where the propensity to carbon formation is enhanced by methane decomposition, resulting in carbon deposition on the catalyst. This will not only deactivate the catalyst but will also produce CO_2 in the AR, which is emitted via the depleted air stream, lowering the CCR of the MA-CLR plant. As the permeate pressure is further increased, more H_2 is available as less product can be recovered due to the lower driving force across the membranes. This results in a system where all OC is reduced in the freeboard zone and a large H_2 content is present in the FR preventing methane decomposition. However, due to the large excess of H_2 leaving the reactor, the CO_2-rich product stream from the fuel reactor will contain large amounts of H_2. Separate from the CO_2 purity constraint, the H_2 in the offgas is not utilized for either heat export or captured as product, therefor lowering the overall energy efficiency of the MA-CLR plant. From an H&MB and thermodynamic perspective a low permeate pressure is preferred. In the next section a similar analysis is performed for the MA-SER plant with respect to material selection, carbon formation, thermodynamic analysis and a sensitivity study on the H&MB integrated network.

Carbon formation in the MA-SER process

Just like the thermodynamic analysis conducted for stable carbon formation in MA-CLR and MA-SMR processes, the stable carbon formation regime shift towards higher H_2O/CH_4 ratios is also observed when H_2 is removed *in situ* for the MA-SER process. This effect is represented in Figures 8A, B as a function of temperature, pressure, HRF and H_2O/CH_4 for the MA-SER process using CaO as sorbent. However, in this case the carbon is effectively removed in the form of CO_2 through the carbonation reaction with CaO, unlike MA-SMR and MA-CLR processes where

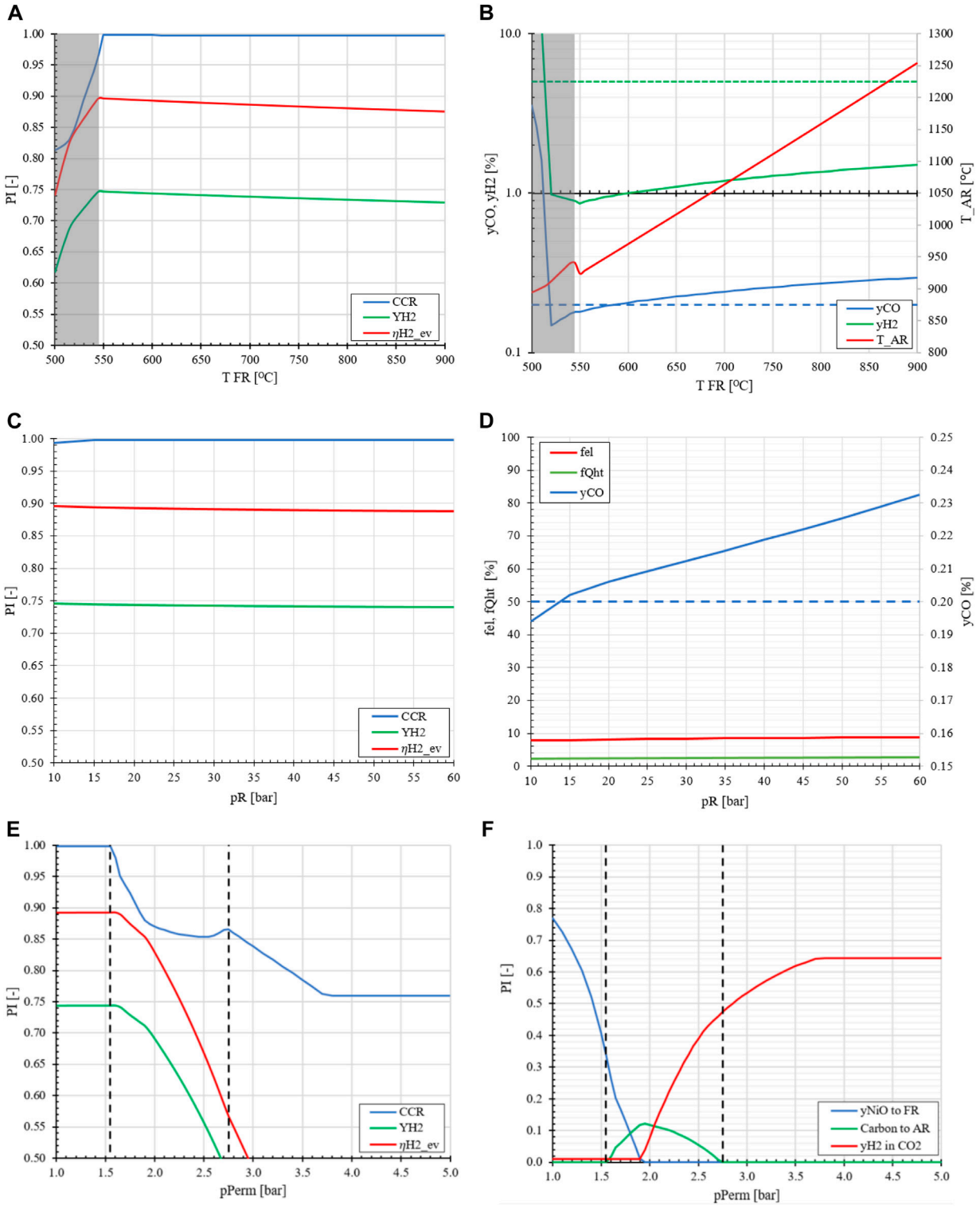

FIGURE 7
The effect of FR temperature **(A, B)**, retentate/reactor pressure **(C, D)** and permeate pressure **(E, F)** on the performance indicators and energy utilization compared to the base case MA-CLR of T_R = 600°C, p_R = 20 bar, p_{Perm} = 1.0 bar and H2O/CH4 = 2.0.

the carbon content in the system increases. The removal of CO_2 results in a reduction of the carbon content as the presence of lower amounts of gaseous CH_4 and CO is observed, required for the MD and rB reaction to be prevalent. This ensures that the minimum H_2O/CH_4 ratios for stoichiometric conversion using combined SMR and WGS reactions are never exceeded, regardless of temperature and pressure. Therefore, there is no need to consider for a minimum H_2O/CH_4 ratio when evaluating of the MA-SER process with

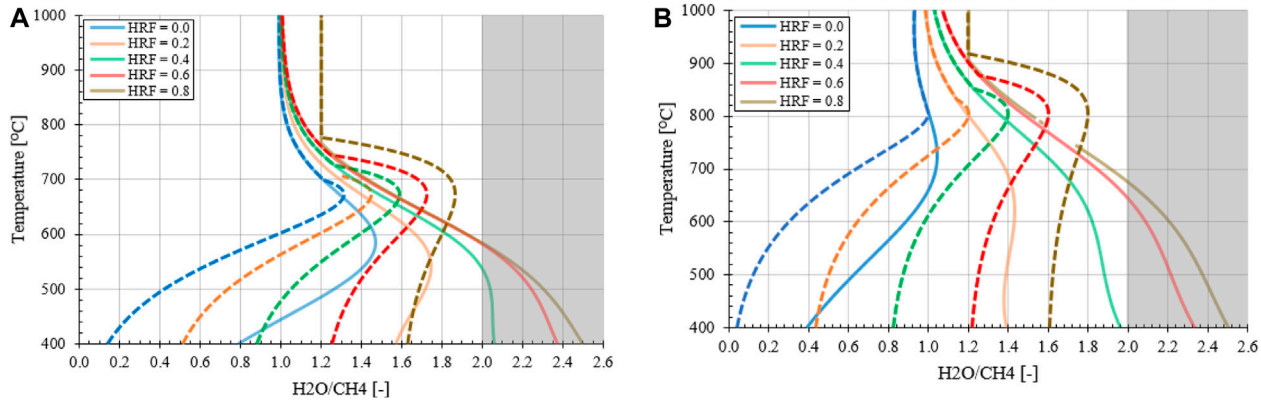

FIGURE 8
(A) Effect of hydrogen removal *in situ* on the shift of stable carbon formation regime, expressed in H_2O/CH_4 ratio, evaluated at 1.0 bar pressure and **(B)** 10 bar. (-) MA-SMR process and (--) for MA-SER process boundary for stable carbon formation. Shaded area is representative of stoichiometric H_2O/CH_4 ratio of 2:1 for maximum hydrogen yield without thermodynamic limitations.

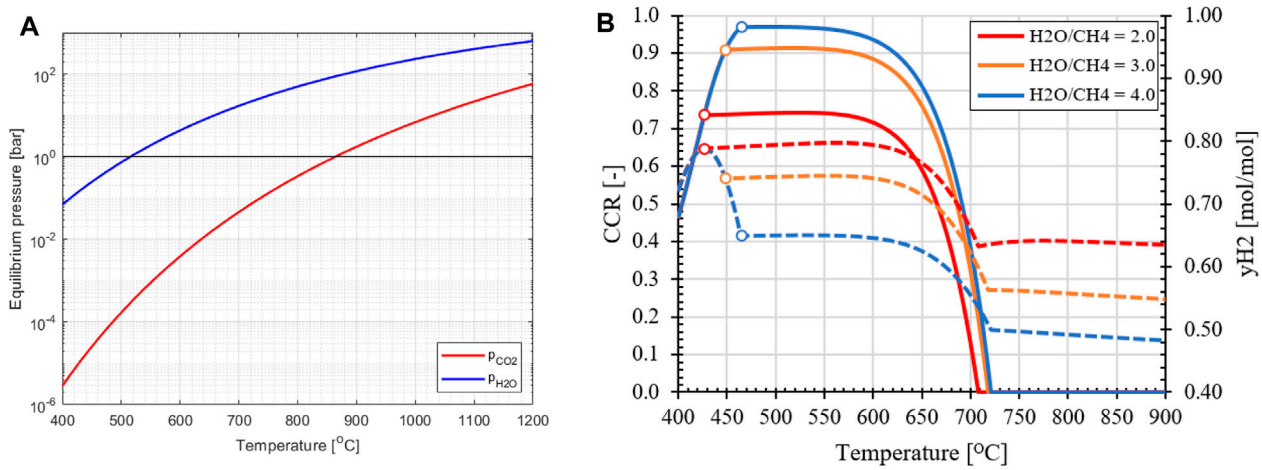

FIGURE 9
(A) Partial pressure at thermodynamic equilibrium for carbonation/calcination reaction with CaO (red) and hydration/dehydration reaction (blue) as function of operation temperature. **(B)** Effect of H_2O/CH_4 ratio on CCR and hydrogen fraction at equilibrium for reference SER process at 1.0 bar pressure. At the right domain from (o) zero $Ca[OH]_2$ is present in equilibrium mixture.

regards to carbon formation. Similar to the MA-CLR process, a preliminary thermodynamic analysis is conducted on the MA-SER system to examine the impact of H_2O/CH_4 ratio, pressure, and temperature on the optimal operating conditions for the plant in relation to Y_{H2} and CCR.

First, the effects of temperature, pressure and H_2O/CH_4 ratio on the KPIs of the standard SER process are evaluated. Based on equilibrium data for the carbonation/calcination reaction shown in Figure 9A, it can be concluded that the CO_2 partial pressure for calcination is unaffected by the reactor pressure, which is the same for the reformer (REF) and regenerator (REG) reactors. Therefore, to operate the REG reactor and reduce the partial pressure of CO_2 for calcination to occur, the REG temperature needs to be increased and/or a larger amount of steam as carrier gas has to be used as feedstock. However, this would result in an increased amount of H_2 being sent to the burner to heat up the H_2O to the regenerator and the solids, effectively reducing the hydrogen yield. Another factor that significantly affects the equilibrium composition of the reformer reactor is the H_2O/CH_4 ratio, as shown in Figure 9B. Increasing the steam excess leads to higher methane conversion, as per Le Chatelier's principle, which shifts the equilibrium composition towards greater H_2 production. It should be noted that due to the excess steam in the feedstock, a lower partial pressure of H_2 is obtained in the reformer, which affects the driving force across the membrane for *in situ* product extraction. With regard to the REF temperature, two regimes can be distinguished. At low REF temperatures, the selectivity of H_2O favors thermodynamically the hydration of CaO (R8) compared to the reforming of CH_4 through the SMR reaction and the carbonation of the formed CO_2 in the process (R7), as shown in Figure 10A. Consequently, a decline in CCR is observed as the temperature decreases, starting from 500°C. This effect is

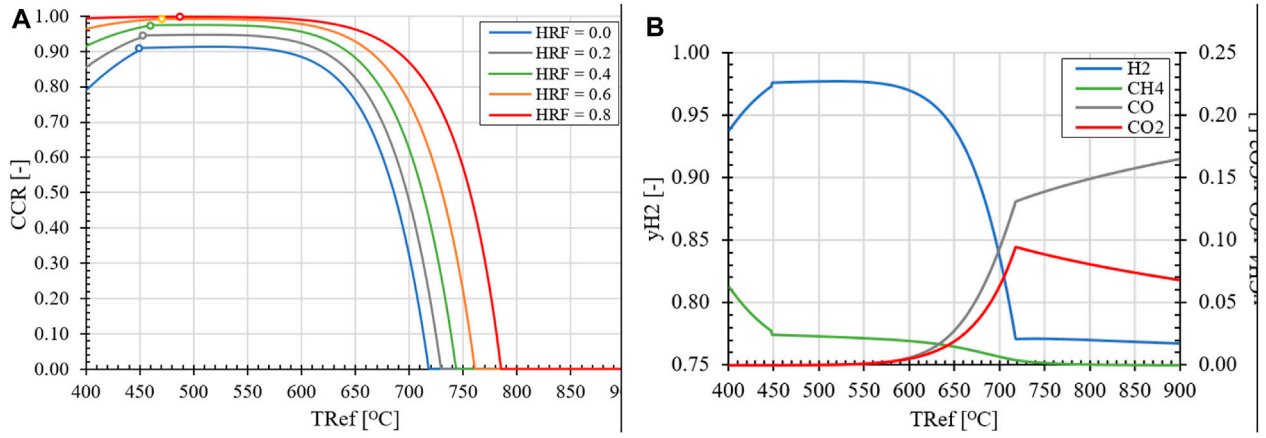

FIGURE 10
(A) Effect of reformer temperature and HRF on CCR for (MA-)SER reactor for H_2O/CH_4 = 3.0, p_R = 1.0 bara. (o) zero $Ca[OH]_2$ formation **(B)** Effect of reformer temperature on the dry product composition of SER for H_2O/CH_4 = 4.0 and p_R = 1.0 bara.

more pronounced at higher H_2O/CH_4 ratios and higher HRFs in the case of the MA-SER process, due to the increase in the partial pressure of H_2O caused by excess steam that is unable to react and/or the removal of products. At higher temperatures, the increase in the equilibrium partial pressure of CO_2 for the carbonation reaction results in a lower CCR, as less CO_2 in the reformate can be captured by the CaO.

Considering these factors, a base case is defined for the MA-SER plant analysis with T_{ref} = 600°C, p_R = 1.0 bar, H_2O/CH_4 = 3.0 and CaO/CH_4 = 1.0. The design specifications for the MA-SER plant will be discussed in the following section.

The H&MB integrated system of the MA-SER process for this study is presented in Figure 11. Similar to the MA-CLR process, a set of design specifications is implemented to limit the number of free variables in the system and constrain the operation window. These design specifications are listed in In Supplementary Appendix SB the composition, temperature and pressure of the individual streams, indicated by the stream number in Figure 11, are presented for the basecase of the MA-SER process in this study.

Table 10, and discussed below:

1. The inlet H_2O/CH_4 ratio for the REF reactor is determined by a stream that combines fresh H_2O feed and the recycle stream obtained from steam condensation, produced as a result of fuel combustion in the burner and excess feed. Depending on the recycle stream flow rate the fresh H_2O feed is adjusted accordingly to meet the desired criteria.
2. In the case of integrated membranes, a driving force is required to extract hydrogen from the reformate stream in the REF reactor *in situ*. To maintain a significant driving force throughout the reactor, the permeate pressure is set to be 0.1 bar lower than the hydrogen partial pressure at the outlet of the REF reactor.
3. To achieve a lower regeneration temperature for the calcination of the sorbent, a stream of steam is introduced to lower the partial pressure of the CO_2 in the regenerator reactor. This steam is recovered after condensation in a steam cycle. The steam inlet to the regenerator is adjusted to achieve a 50/50 CO_2/H_2O molar composition at the outlet of the regenerator reactor.
4. The design operating conditions for the regenerator and the choice of a steam cycle are finalized by lowering the regenerator temperature. The temperature is determined solely based on the reactor pressure and is calculated using the Baker equation. To operate with a potential difference for the calcination reaction, a temperature difference of +Δ10°C is used. The Baker equation, which describes the CO_2 equilibrium, is presented below (Baker et al., 2013):

$$T_{eq}^{CaL} = \frac{8308}{7.079 - \log_{10}(p_{CO2})} \quad [K] \quad (24)$$

5. In the regenerator reactor, a highly endothermic calcination reaction takes place at high temperature to release CO_2 from the sorbent. To minimize the amount of excess hydrogen required to reach such high temperatures and improve the overall process efficiency, the burner temperature is set to be 20°C higher than the regenerator temperature.
6. The burner is supplied with excess oxygen to ensure efficient combustion of the retentate gas from the REF reactor, which contains reductive gases such as H_2, CO, and CH_4. The excess oxygen level is maintained at 20% above the stoichiometric amount required for complete combustion by adjusting the air inlet to the burner.

In Supplementary Appendix SB the composition, temperature and pressure of the individual streams, indicated by the stream number in Figure 11, are presented for the basecase of the MA-SER process in this study.

Sensitivity analysis MA-SER process

In the preliminary analysis, it was determined that the effect of reformer temperature, retentate pressure, and HRF significantly impact the performance of the plant. The reformer temperature

10.3389/fceng.2024.1294752

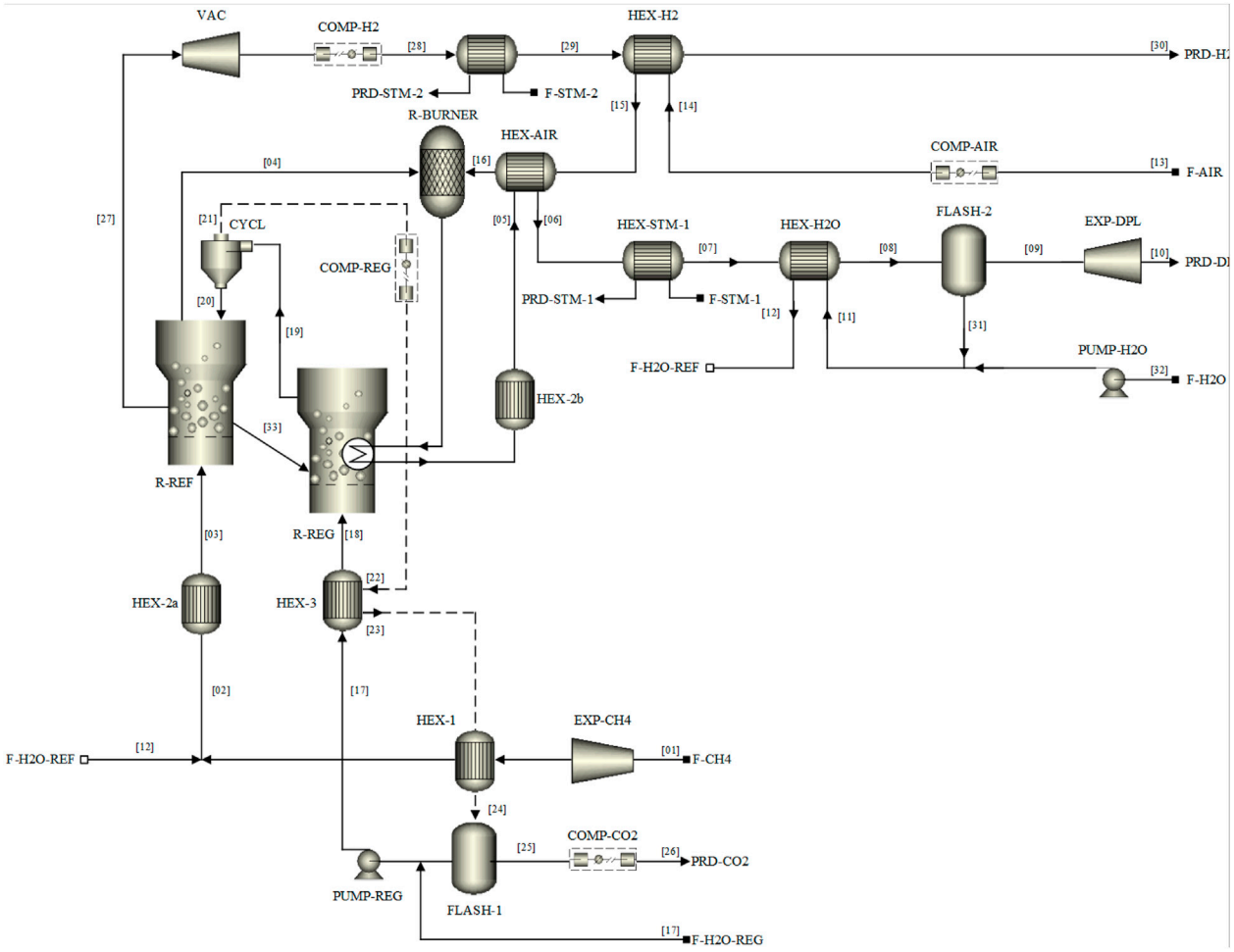

FIGURE 11
M&HB integrated network of the MA-SER plant for hydrogen production.

TABLE 10 Design specs for MA-SER plant in ASPEN Plus.

Design spec	Formula	Variable parameter
Inlet H_2O/CH_4 ratio	$\frac{F_{H2O}}{F_{CH4}}\|_{REF} - \text{Target} = 0$	F-H2O
Driving force membranes	$\frac{Y_{H2}P_{Ret.}}{0.1p_{perm}} - 1 = 0$	pPerm
Driving force calcination 1 Carrier gas	$\frac{F_{CO2}}{F_{H2O}}\|_{REG} - 1 = 0$	F-H2O-REG
Driving force calcination 2 Calcination temperature	$\frac{T_{REG} - T_{eq}^{CaL}}{20} - 1 = 0$	TR REG
Calcination energy	$\frac{-Q_{burn}}{Q_{REG}} - 1 = 0$	HRF
Oxygen-to-fuel ratio	$\frac{F_{O2}}{2F_{CH4}+0.5F_{CO}+0.5F_{H2}}\|_{BURN} - 1.2 = 0$	F-AIR

can be regulated by the balancing the steam export in relation to the HRF. The retentate pressure is a variable that can be adjusted within the system. Additionally, the CaO utilization is a factor related to the efficiency of energy integration, as it is linked to reaction rate of the gas-solid reaction and associated heat consumption in the system.

An increase in the REF temperature has a negative effect on the CCR, as can be observed in Figure 12A. From a thermodynamic perspective the equilibrium partial pressure of CO_2 in the REF increases with temperature, reducing the amount of CO_2 reacting with CaO. When focusing on the energy integration of the system, a lower temperature difference between the REF and REG reactor results in a lower heat demand from the burner to the heat up the solids. This reduces the amount of fuel needed in the burner leading to an increase in the achieved Y_{H2}. A secondary effect of reducing the temperature difference between the reactors is the decrease in the amount of high-temperature energy required to heat streams to their desired high temperatures. This

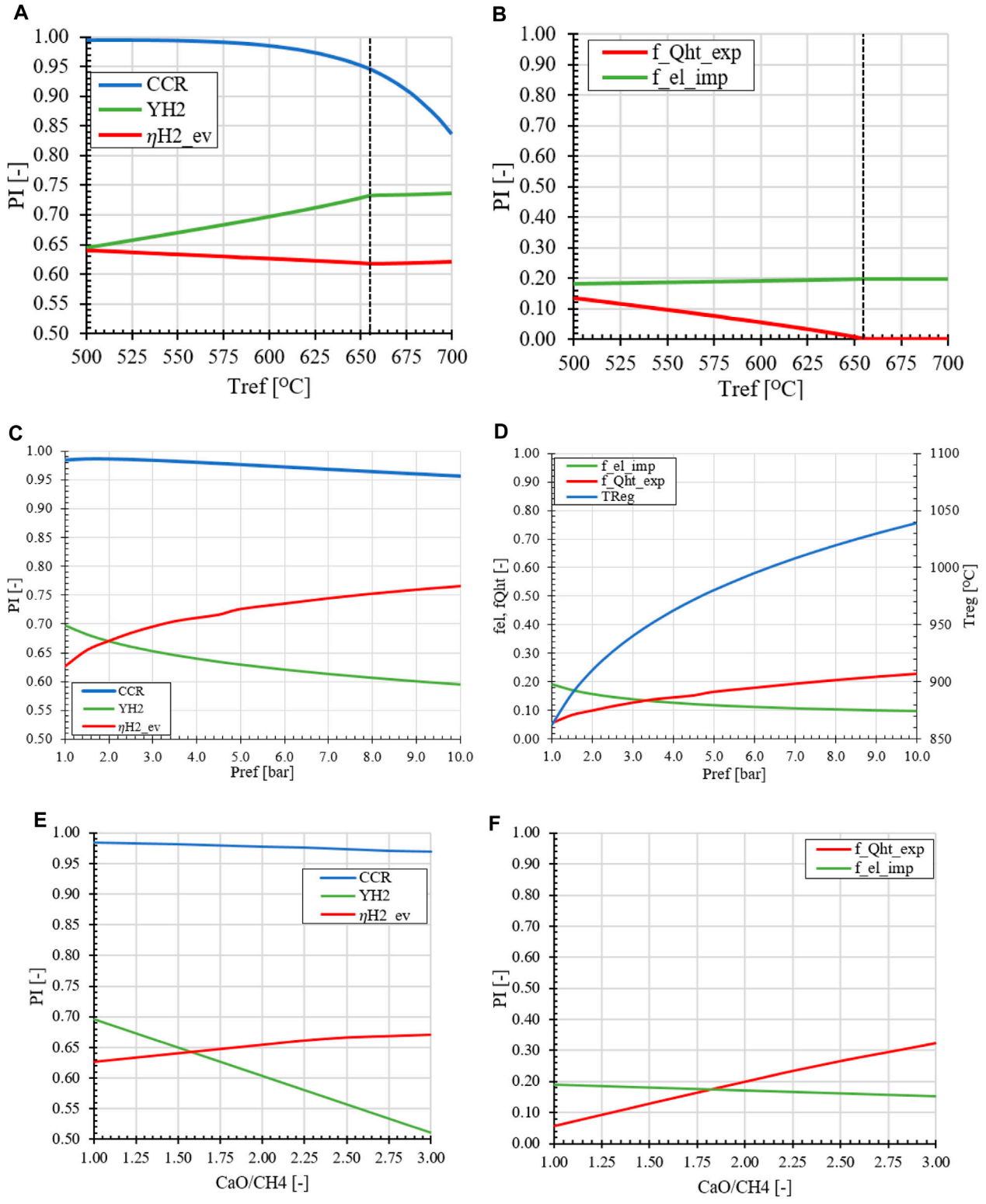

FIGURE 12
Effect of operation parameters on the MA-SER performance indicators **(A, B)** Reformer temperature **(C, D)** Retentate pressure **(E, F)** sorbent circulation rate compared to the base case of T_{ref} = 600°C, p_R = 1.0 bar, H_2O/CH_4 = 3.0 and CaO/CH4 = 1.0.

results in a lower demand for excess energy, which would otherwise be exported in the form of LP steam. This is reflected in Figure 12B where a slight increase in electricity import can be seen at higher reformer temperatures due to a significant increase in the hydrogen yield.

In the second case, the effect of the pressure in the MA-SER system is investigated. From a thermodynamic perspective, the pressure has three main effects on the MA-SER process: (1) At higher pressures, the CO_2 gas fraction in the REF reactor can be

lower, effectively increasing the CCR while recovering H_2 from the reformate stream. (2) The negative effect of pressure on the SMR reaction in the REF reactor is suppressed by the *in situ* removal of H_2. This results in an overall higher CCR, as presented in Figure 12C. (3) However, the higher pressure in the REG reactor requires a significantly higher calcination temperature to liberate the CO_2 from the sorbent, as shown in Figure 12D. The effect of pressure is reflected in the energy demand of the plant and the product distribution between hydrogen as product and as fuel (Y_{H2} vs. f_{Qt}^{exp}). With an increase in high-temperature heat demand to heat up the solids, a large excess of high-temperature heat is generated in the plant without the ability to utilize this stream in other parts of the plant. Thus, to improve the energy efficiency of the plant, the excess heat is used to produce LP steam and exported, as depicted in Figure 12D. As more H_2 is sent to the burner at higher REG temperatures, a larger amount of hydrogen is used as fuel compared to the amount obtained as product. This is evident in the negative trend of Y_{H2} and the positive trend in η_{H2}^{ev} in Figure 12C.

Considering economic motivations, an increase in pressure has implications for both OPEX and CAPEX. Due to the higher operating temperature and pressure in the REF reactor, it is necessary to carefully select suitable building materials that can withstand oxidative conditions. While the REF reactor benefits from the increase in operation pressure, the REG reactor faces challenges in terms of design and operation under these conditions. Increasing the pressure results in a higher flux for the membranes in the REF reactor, decreasing the required membrane area. This, in turn, leads to a decrease in the size of the reactors and equipment, as the volumetric flow rate of gasses is reduced. However, it is important to strike a balance between the desired product distribution (Y_{H2}, CCR, and η_{H2}^{ev}) and equipment costs in order to achieve an optimal H_2 cost. Both factors should be considered in the overall economic analysis of the MA-SER system.

One of the main parameters in the design of the MA-SER hydrogen plant is the sorbent utilization in the reformer reactor. From both thermodynamic and plant performance perspectives, a CaO/CH_4 ratio of 1.0 is considered desirable. This means that all sorbent material introduced facilitates in the capture of the CO_2 produced *in situ*. When the CaO/CH_4 ratio is increased, it leads to an increase in the solids circulation rate between the reformer and regenerator, resulting in a heat sink in the process. As more solid material is sent from a low temperature REF reactor to the REG reactor operated at high temperature, a higher heat demand for heating excess material is required without the benefit of capturing more CO_2 in the process. This extra energy demand for the solid material is supplied by the burner. This extra thermal energy demand is acquired by sending more H_2 to the burner, reducing the overall hydrogen production yield. This effect is shown in Figures 12E, F. The excess hydrogen which is converted into high temperature heat is recovered using heat exchangers and is exported as steam, which is reflected by the equivalent hydrogen efficiency and also by the fraction energy export steam vs. hydrogen product.

As described in the introduction, two different rate limiting mechanisms are present during the carbonation of the CaO grains. At higher sorbent conversions, the carbonation reaction rate becomes diffusion limited, meaning that the carbonation reaction is significantly reduced. On the other hand, operating the reformer reactor at the kinetically reaction rate limiting regime requires a lower sorbent conversion, which can be accomplished by increasing the solids circulation rate and consequently increasing the CaO/CH_4 feed ratio. This trade-off between reactor size and hydrogen yield requires further investigation to determine the optimal hydrogen cost using a techno-economic analysis. To improve the process, the kinetically limited regime must be extended as much as possible by improving the chemical- and structural properties of the sorbent.

In the next section, the optimal operation conditions for both MA-SER and MA-CLR processes are compared to evaluate the benefits of each process depending on the desired optimal performance indicator. The optimal process conditions for the MA-SER process are selected and compared to the those for the MA-CLR plant.

MA-CLR and MA-SER performance comparison

The evaluation of the best cases for both the MA-CLR and MA-SER hydrogen plants is presented in Table 11. Examining the key performance indicators, Y_{H2} and CCR, it is evident that the MA-CLR process achieves a significantly higher hydrogen yield compared to the optimal operation conditions of the MA-SER system. This discrepancy can be attributed to the balance created in the MA-SER process between the amount of H_2 used as fuel in the burner and the amount recovered as chemical product. In contrast, the MA-CLR process utilizes hydrogen as a reducing agent for the OC in the freeboard zone. This distinction is reflected in the fraction of energy export in the form of LP steam, which is higher for the MA-SER process compared to the energy potential in the hydrogen product stream. Reducing the temperature difference between the REF and REG reactors improves energy management, as less energy is required to heat up the solids. However, increasing the pressure in the reactors necessitates a higher REG temperature to liberate CO_2 for the calcination reaction to occur. One advantage of the MA-SER process over to the MA-CLR process is the quality of the CO_2 product stream. In the MA-CLR process, the CO_2-rich stream contains traces of reformate gasses, whereas in theory, the MA-SER process yields a purer CO_2 stream after moisture removal. However, in the MA-SER process, direct CO_2 emissions to the environment are a result of the process design, while in the MA-CLR process, the carbon stream is enclosed, preventing emissions.

Another key parameter to consider is the equivalent CCR, which takes into account the emission taxes and the energy penalty associated with the CO_2 separation from the product streams. Exporting steam provides a positive contribution as the associated CO_2 emissions are reduced due to carbon capture in both the MA-SER and MA-CLR processes. However, there is a negative contribution associated with the electricity import, mainly for the use of compressors. It is assumed that methane combustion is used to generate electricity, implying that CO_2 emissions are associated with the production at an external location. In the case of the MA-SER plant, the relatively high electricity consumption, compared to the MA-CLR process, is a result of

TABLE 11 Comparison of optimal operation conditions for MA-SER and MA-CLR hydrogen plant based and corresponding performance parameters for H&MB integrated systems.

Process parameters	Dimension	MA-SER				MA-CLR			
Tref/Tfuel	[°C]	500	600	500	600	600			
Treg/Tair	[°C]	862.7		980.4		970.2			
pRet	[bar]	1.0		5.0		20		40	
pPerm	[bar]	0.48	0.44		2.74	1.0			
O_2/CH_4	[−]	0.71	0.61	0.86	0.74	0.51	0.53	0.51	0.54
H_2O/CH_4	[−]	3.0				2.0	3.0	2.0	3.0
Performance indicators									
$\mathbf{Y_{H2}}$	[−]	**0.644**	**0.697**	**0.570**	**0.629**	**0.744**	**0.730**	**0.741**	**0.726**
CCR	[−]	**0.994**	**0.985**	**0.931**	**0.977**	**0.998**	**0.998**	**0.998**	**0.998**
CCR^{ev}	[−]	0.743	0.622	0.979	0.910	0.865	0.881	0.858	0.874
yCO	[%]	-	-	-	-	0.21	0.16	0.22	0.17
yH2	[%]	-	-	-	-	1.00	1.53	0.99	1.52
η_{H2}	[−]	0.773	0.836	0.863	0.755	0.893	0.876	0.890	0.872
$\mathbf{\eta_{H2}^{ev}}$	[−]	**0.640**	**0.627**	**0.736**	**0.726**	**0.791**	**0.777**	**0.783**	**0.766**
E_{CO2}	$\left[\frac{kg_{CO2}}{GJ_{H2}}\right]$	0.4	1.0	5.6	1.7	-	-	-	-
$\mathbf{E_{CO2}^{ev}}$	$\left[\frac{kg_{CO2}}{GJ_{H2}}\right]$	**18.3**	**24.9**	**1.7**	**6.2**	**8.2**	**7.4**	**8.7**	**7.8**
f_{el}^{imp}	[%]	18.0	19.1	11.0	11.7	8.1	8.2	8.6	8.6
f_{Qht}^{exp}	[%]	13.5	5.6	25.4	16.6	2.4	4.0	5.6	4.4

The bold character is to emphasize these results as main objective KPIs.

the significant number of pressure manipulations required in the process. The CO_2 emissions related to the significant electricity import is partially offset by the export of LP steam. It can be concluded from the fraction of energy import/export that the MA-CLR is more energy integral compared to the MA-SER plant, and thus less dependent on external energy infrastructure and suitable in locations with constraints on energy availability.

Outlook on the MA-SER and MA-CLR techno-economic evaluation including CAPEX parameters and dimensioning of equipment

The plant design and commissioning is not only based on the optimal KPIs discussed in the previous section, which is mostly focused on OPEX derived parameters. To evaluate the optimal hydrogen production capacity, based on the hydrogen market demand and price, the selection of material and dimensioning of the equipment the CAPEX KPIs must be included. These KPIs are related to upfront investment in design-, construction- and installment cost, initial material- and equipment cost and depreciation of equipment. CAPEX KPIs that must be included in the techno-economic evaluation must include but are not limited by: return of investment, utilization rate and the depreciation of assets.

One of the major aspect, based on the desired production capacity, is the dimensioning of the reactors and the auxiliaries. The dual fluidized bed membrane reactor models for describing the MA-SER and MA-CLR process used in this study are based on thermodynamic equilibrium and do not include the complexity of hydrodynamic interactions or mass- and heat transfer limitations. Also the mechanical- and chemical degradation of the solid material due to fluidization and transfer between the reactors operating at different conditions are not included. This negatively affects the reaction rate kinetics over time and also the fluidized bed behavior due to the particle size distribution shift trough particle abrasion if not mitigated by a sufficient material renewal rate and the removal of spend material. With respect to the membranes it must be noted that multiple factors are affecting the performance based on the selected operation conditions and geometry. These are affecting the local membrane permeate flux, resulting from a combination of mass transfer limiting steps; such as competitive adsorption on the membrane surface, concentration polarization due to limited H2 diffusion from the gas phase to the membrane surface and/or bypass of bubbles through preferential flow pathing through the membrane submerged manifold. In particular the hydrodynamic interaction of suspended membranes in a fluidized bed must be properly assessed. To dimension the fluidized bed reactors

adequately a phenomenological model (Kunii, 2001) or a two fluid model (TFM) (Helmi et al., 2018) can be used. These models included the effects of reaction kinetics and hydrodynamic interactions of gas-solid systems on both heat- and mass transfer. This can be used to identify the rate limiting step and optimize the design. In addition to CLR and SER kinetics the MD, rB reaction kinetics can be incorporated to ensure that carbon formation at localized conditions is prevented. This model and resulting process streams can be used as input to improve on the H&MB integrated network for further optimization.

Conclusion and recommendations

A thorough analysis was conducted on the performance of MA-SER and MA-CLR plants for hydrogen production. The preliminary thermodynamic analysis focused on the impact of *in situ* hydrogen removal on the shift in the stable carbon formation regime shift for the MA-SMR, MA-CLR and MA-SER processes under various operating conditions, including reactor temperature, pressure, H_2O/CH_4 ratios, and HRF. The findings revealed that selectively removing hydrogen *in situ* as a reductive gas enhances the propensity for carbon formation at lower reforming temperatures in both the MA-SMR and MA-CLR processes. This surpassed the stoichiometric H_2O/CH_4 ratio for MA-SMR process and the autothermal conditions required for ideal conditions in the MA-CLR process. In the case of the MA-SER process, carbon removal in the form of CO_2 through the continuous carbonation reaction with CaO led to a shift in the carbon formation regime below the stoichiometric ratio of H_2O/CH_4 = 2.0 under all considered operating conditions.

To facilitate a comparison between the two processes, which are capable of operating under different operation conditions, performance indicators relating to mass and energy utilization are defined. The critical performance indicators include CCR, Y_{H2} and η^{ev}_{H2}. Both the MA-CLR and MA-SER processes are simulated using ASPEN® Plus V10, and a sensitivity study is conducted based on the preliminary analysis and process description. Additionally, the impact of operating conditions on the techno-economic aspect is thoroughly discussed. This analysis aims to provide a comprehensive understanding of the motivation behind studying these specific effects and their influence on the plant design and hydrogen cost.

The base case for the MA-CLR process involves the following parameters:
T_{FR} = 600 °C, p_R = 20 bar, p_{perm} = 1.0 bar, H_2O/CH_4 = 2.0. The effects of the fuel reactor temperature, reactor pressure and permeate pressure were investigated. Increasing the fuel reactor temperature has two notable effects. The temperature range can be divided into two domains: an unstable region below 550°C where carbon formation is thermodynamically favored, and a stable operating regime above this temperature. When the FR temperature is increased from 600°C to 800°C, the Y_{H2} and CCR decrease slightly from 0.744 to 0.998 to 0.734 & 0.997, respectively. Therefore, it can be concluded that the effect of FR temperature does not significantly affect the primary performance indicators above a critical temperature. However, it is important to note that as the FR temperature increases, the AR temperature also increases, which affects the quality of the CO_2-rich stream with respect to trace amounts of CH_4, CO and H_2. The reactor pressure does not have a significant effect on the performance indicators of the MA-CLR plant. This is because the reactions in the FR and AR with respect to the OC are irreversible. Increase the pressure from 20 to 60 bar leads to a minor decrease in Y_{H2} of 0.744 to 0.740, while the CCR remains constant at 0.998. The effect of reactor pressure will be represented in the sizing of the reactor, membrane and auxiliary equipment. The permeate pressure is a free variable in the system as this controls the amount of (partial) reduction of the OC in the FBZ, controlling the amount of oxygen content entering the FR available for the catalytic reforming. A permeate pressure below 1.5 bar is required to operate in a regime with sufficient oxygen content in the FR to prevent stable carbon formation on the OC.

The base case for the MA-SER process is T_{ref} = 600 °C, p_R = 1.0 bar, H_2O/CH_4 = 3.0, CaO/CH_4 = 1.0 and the effect of reformer reactor temperature, reactor pressure and solid circulation rate is investigated in the sensitivity analysis. Increase of the reformer temperature has two significant effects, it lowers the CCR as the equilibrium partial pressure for carbonation is increased but also reduces the temperature difference between the reformer and regenerator reactor. This reduces the energy demand for the burner to heat-up the solids from the reformer to the regenerator in order to perform the calcination reaction. There for less hydrogen has to be send to the burner, for the effectively induced heat-sink, and increases the hydrogen yield. From a techno-economic perspective it must be considered that a lower reformer temperature results in lower catalytic and gas-solid kinetics, increasing the required reactor size for the same feedstock. Increasing the REF temperature from 600°C to 700°C reduces the CCR significantly from 0.985 to 0.837 at an increasing Y_{H2} from 0.697 to 0.736. Increase of the reactor pressure contributes to benefits for the REF reactor with respect to increased membrane flux, lower CO_2 content in the reformate and smaller reactor size while introducing limitations in the REG reactor with respect to the liberation of CO_2 due to increased calcination temperature. An increase of high temperature heat demand for the heat-up of the solids, a large excess of high value high temperature heat is present without the ability to utilize this stream in other sections of the plant. Therefor to increase the energy efficiency of the plant the excess heat is used to produce MP to LP steam and exported. This effect is represented in the Y_{H2} and η^{ev}_{H2} when increasing the reactor pressure from 1.0 to 10 bar, being 0.697 and 0.627 to 0.629 and 0.726 respectively while the CCR not significantly affected, from 0.985 to 0.957. The effect of sorbent utilization is investigated with respect to the performance indicators due to the implication of sorbent kinetics. The sorbent is affected by the conversion of the CaO grains, changing from a fast surface reaction kinetics at low conversion to a slow carbonation rate determined by the ion diffusion rate limited regime at high conversions. Increasing the CaO/CH_4 ratio effectively increasing the solid circulation rate between the reformer and regenerator, generating a heatsink in the process. This extra thermal energy demand is acquired by sending more hydrogen to the burner, reducing the Y_{H2} overall. Increasing the CaO/CH_4 feed ratio from 1.0 to 3.0 reduces the Y_{H2} significantly from 0.697 to 0.510 while the CCR is slightly affected, from 0.985 to 0.969.

Comparing the MA-SER and MA-CLR processes based on the M&HB optimal cases it can be concluded that the MA-CLR process

outperforms the MA-SER plants on multiple performance indicators. Comparing the Y_{H2} for the best MA-SER case with a comparable CCR the MA-CLR process has a 2.9%–6.2% lower hydrogen yield. This conclusion is further underpinned by the fact that, compared to the overall energy utilization of the plant where hydrogen is seen as energy carrier, to be 62.7%–73.6% at best for the MA-SER process compared to 76.6%–79.1% for the MA-CLR plant. The difference of hydrogen yield for the MA-SER process to the MA-CLR process is explained by the fact that hydrogen is used as fuel in the burner to supply the heat for the endothermic reaction at high temperature in the regenerator reactor compared to oxygen carrier as fuel in the air reactor where hydrogen is used as reductive gas in the freeboard zone and the hot (partially) reduced oxygen carrier is used for the endothermic reforming reaction. This effect is enhanced by using the hot fluegas from the FR for the energy demand in the pre-reformer reactor stage in the MA-CLR process. One of the major benefits of the MA-SER process compared to the MA-CLR process is the purity of the CO_2 product stream. In the case of MA-SER the CO_2 is theoretically pure compared to the MA-CLR product stream which contains significant amounts of reformate gasses, such as CO, H_2 and CH_4. Depending on the application of the CO_2, a further post-processing step is required for the MA-CLR plant, reducing the plant energy efficiency. It must be noted that the success for deployment for these hydrogen production plants for either one of the processes is fully dependent on the chemical and mechanical stability of (1) the perm-selective membranes and (2) the solids. A phenomenological fluidized bed reactor model or a TFM model, incorporating both hydrodynamic and reaction kinetic effect, can be used to dimension the DFBR and incorporate the predicted process stream for the H&MB design improvement in this study. A techno-economic analysis is required to determine the optimal size and location of the hydrogen plant, centralized or decentralized, and a balance between CCR, Y_{H2} and energy export/import for the minimum hydrogen production cost.

Data availability statement

The raw data supporting the conclusion of this article will be made available by the authors, without undue reservation.

Author contributions

SP: Conceptualization, Formal Analysis, Investigation, Methodology, Software, Writing–original draft. MB: Conceptualization, Formal Analysis, Investigation, Methodology, Software, Validation, Writing–review and editing. FG: Conceptualization, Funding acquisition, Supervision, Writing–review and editing. MV: Conceptualization, Funding acquisition, Supervision, Writing–review and editing.

Funding

The author(s) declare financial support was received for the research, authorship, and/or publication of this article. This project has received funding from the European Union's Horizon 2020 research and innovation program under grant agreement No. 760944 (MEMBER project).

Conflict of interest

The authors declare that the research was conducted in the absence of any commercial or financial relationships that could be construed as a potential conflict of interest.

Publisher's note

All claims expressed in this article are solely those of the authors and do not necessarily represent those of their affiliated organizations, or those of the publisher, the editors and the reviewers. Any product that may be evaluated in this article, or claim that may be made by its manufacturer, is not guaranteed or endorsed by the publisher.

Supplementary material

The Supplementary Material for this article can be found online at: https://www.frontiersin.org/articles/10.3389/fceng.2024.1294752/full#supplementary-material

References

Abad, A. (2015). *Chemical looping for hydrogen production*. Amsterdam, Netherlands: Elsevier.

Abanades, J. C., Rubin, E. S., and Anthony, E. J. (2004). Sorbent cost and performance in CO2 capture systems. *Ind. Eng. Chem. Res.* 43 (13), 3462–3466. doi:10.1021/ie049962v

Anantharaman, C. E. R., Bolland, O., Booth, N., and van Dorst, E. (2011). *Enabling advanced pre-combustion capture techniques and plants*. Brussels, Belgium: European Commission.

Annesini, M. C., Piemonte, V., and Turchetti, L. (2007). Carbon Formation in the steam reforming process: a thermodynamic analysis based on the elemental composition. *Chem. Eng. Trans.* 11, 21–26.

Arku, P., Tasnim, S. H., Mahmud, S., and Dutta, A. (2020). Numerical investigation of the effects of coke on transport properties in an oxidative fuel cell reformer. *ACS Omega* 5 (44), 28555–28564. doi:10.1021/acsomega.0c03251

Arratibel, A., Medrano, J. A., Melendez, J., Pacheco Tanaka, D. A., van Sint Annaland, M., and Gallucci, F. (2018). Attrition-resistant membranes for fluidized-bed membrane reactors: double-skin membranes. *J. Memb. Sci.* 563, 419–426. doi:10.1016/j.memsci.2018.06.012

Arstad, B., Prostak, J., and Blom, R. (2012). Continuous hydrogen production by sorption enhanced steam methane reforming (SE-SMR) in a circulating fluidized bed reactor: sorbent to catalyst ratio dependencies. *Chem. Eng. J.* 189–190, 413–421. doi:10.1016/j.cej.2012.02.057

Bacquart, T., Arrhenius, K., Persijn, S., Rojo, A., Auprêtre, F., Gozlan, B., et al. (2019). Hydrogen fuel quality from two main production processes: steam methane reforming and proton exchange membrane water electrolysis. *J. Power Sources* 444, 227170. doi:10.1016/j.jpowsour.2019.227170

Baker, E. H., Sherman, W., Repasky, M., and Beuming, T. (2013). Improved docking of polypeptides with glide. *J. Chem. Inf. Model.* 53 (9), 1689–1699. doi:10.1021/ci400128m

Behnam, M., and Dixon, A. G. (2017). 3D CFD simulations of local carbon formation in steam methane reforming catalyst particles. *Int. J. Chem. React. Eng.* 15 (6), 1–17. doi:10.1515/ijcre-2017-0067

Boon, J., Cobden, P. D., van Dijk, H. A. J., Hoogland, C., van Selow, E. R., and van Sint Annaland, M. (2014). Isotherm model for high-temperature, high-pressure adsorption of and on K-promoted hydrotalcite. *Chem. Eng. J.* 248, 406–414. doi:10.1016/j.cej.2014.03.056

Cannone, S. F., Lanzini, A., and Santarelli, M. (2021). A review on CO2 capture technologies with focus on CO2-enhanced methane recovery from hydrates. *Energies* 14 (2), 387. doi:10.3390/en14020387

Carpenter, S. M., and Long, H. A. (2017). *Integrated gasification combined cycle (IGCC) technologies, ch 13: integration of carbon capture in IGCC systems*. Amsterdam, Netherlands: Elsevier Ltd.

Chhiti, Y., Peyrot, M., and Salvador, S. (2013). Soot formation and oxidation during bio-oil gasification: experiments and modeling. *J. Energy Chem.* 22 (5), 701–709. doi:10.1016/s2095-4956(13)60093-5

Dittmar, B., Behrens, A., Schödel, N., Rüttinger, M., Franco, T., Straczewski, G., et al. (2013). Methane steam reforming operation and thermal stability of new porous metal supported tubular palladium composite membranes. *Int. J. Hydrogen Energy* 38 (21), 8759–8771. doi:10.1016/j.ijhydene.2013.05.030

El-Halwagi, M. M. (2006). *Process integration for sustainable design: systematic tools and industrial applications*. Angra dos Reis, RJ, Brazil: Texas A&M University.

Ewan, B. C. R., and Allen, R. W. K. (2005). A figure of merit assessment of the routes to hydrogen. *Int. J. Hydrogen Energy* 30 (8), 809–819. doi:10.1016/j.ijhydene.2005.02.003

ExxonMobil (2018). 2018 outlook for energy: a view to 2040. https://www.aop.es/wp-content/uploads/2019/05/2018-Outlook-for-Energy-Exxon.pdf.

Fan, L.-S. (2014). *Chemical looping systems for fossil energy conversions*. Hoboken, New Jersey, United States: Wiley.

Feng, B., An, H., and Tan, E. (2007). Screening of CO2 adsorbing materials for zero emission power generation systems. *Energy Fuels* 21 (2), 426–434. doi:10.1021/ef0604036

Gallucci, F., Fernandez, E., Corengia, P., and van Sint Annaland, M. (2013). Recent advances on membranes and membrane reactors for hydrogen production. *Chem. Eng. Sci.* 92, 40–66. doi:10.1016/j.ces.2013.01.008

Gao, J., Wang, Y., Ping, Y., Hu, D., Xu, G., Gu, F., et al. (2012). A thermodynamic analysis of methanation reactions of carbon oxides for the production of synthetic natural gas. *RSC Adv.* 2 (6), 2358–2368. doi:10.1039/c2ra00632d

García-Lario, A. L., Aznar, M., Martinez, I., Grasa, G. S., and Murillo, R. (2015). Experimental study of the application of a NiO/NiAl2O4 catalyst and a CaO-based synthetic sorbent on the Sorption Enhanced Reforming process. *Int. J. Hydrogen Energy* 40 (1), 219–232. doi:10.1016/j.ijhydene.2014.10.033

Harrison, D. P. (2008). Sorption-enhanced hydrogen production: a review. *Am. Chem. Soc.* 47, 6486–6501. doi:10.1021/ie800298z

Helmi, A., Voncken, R. J. W., Raijmakers, A. J., Roghair, I., Gallucci, F., and van Sint Annaland, M. (2018). On concentration polarization in fluidized bed membrane reactors. *Chem. Eng. J.* 332, 464–478. doi:10.1016/j.cej.2017.09.045

IEA (2018). World energy balances: overview. https://www.iea.org/reports/world-energy-balances-overview/world.

IEA (2019). *The future of hydrogen*. Paris, France: IEA.

Jaworski, Z., Zakrzewska, B., and Pianko-Oprych, P. (2017). On thermodynamic equilibrium of carbon deposition from gaseous C-H-O mixtures: updating for nanotubes. *Rev. Chem. Eng.* 33 (3), 217–235. doi:10.1515/revce-2016-0022

Kang, K. S., Kim, C. H., Bae, K. K., Cho, W. C., Kim, S. H., and Park, C. S. (2010). Oxygen-carrier selection and thermal analysis of the chemical-looping process for hydrogen production. *Int. J. Hydrogen Energy* 35 (22), 12246–12254. doi:10.1016/j.ijhydene.2010.08.043

Kunii, L. O. (2001). *Fluidization engineering*. Amsterdam, Netherlands: Elsevier Science.

Lægsgaard Jørgensen, S., Nielsen, P. E. H., and Lehrmann, P. (1995). Steam reforming of methane in a membrane reactor. *Catal. Today* 25 (3–4), 303–307. doi:10.1016/0920-5861(95)00074-p

Li, Z. H., Wang, Y., Xu, K., Yang, J. Z., Niu, S. B., and Yao, H. (2016). Effect of steam on CaO regeneration, carbonation and hydration reactions for CO2capture. *Fuel Process. Technol.* 151, 101–106. doi:10.1016/j.fuproc.2016.05.019

Lugvishchuk, D. S., Kulchakovsky, P. I., Mitberg, E. B., and Mordkovich, V. Z. (2018). Soot Formation in the methane partial oxidation process under conditions of partial saturation with water vapor. *Pet. Chem.* 58 (5), 427–433. doi:10.1134/s0965544118050109

Marcu, A., Elkerbout, M., and Wijnand, S. (2016). 2017 state of the EU ETS report. https://www.i4ce.org/wp-content/uploads/17-05-State_of_eu_ets_report_2017_updated.pdf.

Markets Insider (2021). CO2-european-emission-allowances. https://markets.businessinsider.com/commodities/CO2-european-emission-allowances(19/05/21.

Martínez, I., Romano, M. C., Chiesa, P., Grasa, G., and Murillo, R. (2013). Hydrogen production through sorption enhanced steam reforming of natural gas: thermodynamic plant assessment. *Int. J. Hydrogen Energy* 38 (35), 15180–15199. doi:10.1016/j.ijhydene.2013.09.062

Masson-Delmotte, V., et al. (2019). Global warming of 1.5°C, Summary for policy makers. https://www.ipcc.ch/site/assets/uploads/sites/2/2019/06/SR15_Full_Report_High_Res.pdf.

Medrano, J. A., Fernandez, E., Melendez, J., Parco, M., Tanaka, D. A. P., van Sint Annaland, M., et al. (2016). Pd-based metallic supported membranes: high-temperature stability and fluidized bed reactor testing. *Int. J. Hydrogen Energy* 41 (20), 8706–8718. doi:10.1016/j.ijhydene.2015.10.094

Medrano, J. A., Potdar, I., Melendez, J., Spallina, V., Pacheco-Tanaka, D., van Sint Annaland, M., et al. (2017). The membrane-assisted chemical looping reforming concept for efficient H2production with inherent CO2capture: experimental demonstration and model validation. *Appl. Energy* 215, 75–86. doi:10.1016/j.apenergy.2018.01.087

Medrano, J. A., Spallina, V., Van Sint Annaland, M., and Gallucci, F. (2014). Thermodynamic analysis of a membrane-assisted chemical looping reforming reactor concept for combined H2 production and CO2 capture. *Int. J. Hydrogen Energy* 39 (9), 4725–4738. doi:10.1016/j.ijhydene.2013.11.126

Metz, B., Davidson, O., De Coninck, H. C., Loss, M., and Meyer, L. A. (2005). *IPCC special report on carbon dioxide capture and storage*. Cambridge, England: Cambridge University Press.

Moore, E. J. (1992). *U . S. Geological survey professional paper 1228-E availability of books and maps of the U . S. Geological survey*. Reston, Virginia, USA: United States Geological Survey.

Nakagawa, K., and Ohashi, T. (1999). A reversible change between lithium zirconate and zirconia in molten carbonate. *Electrochemistry* 67 (6), 618–621. doi:10.5796/electrochemistry.67.618

Ockwig, N. W., and Nenoff, T. M. (2007). Membranes for hydrogen separation. *Chem. Rev.* 107 (10), 4078–4110. doi:10.1021/cr0501792

Oertel, M., Schmitz, J., Weirich, W., Jendryssek-Neumann, D., and Schulten, R. (1987). Steam reforming of natural gas with intergrated hydrogen separation for hydrogen production. *Chem. Eng. Technol.* 10 (1), 248–255. doi:10.1002/ceat.270100130

Pedernera, M. N., Piña, J., and Borio, D. O. (2007). Kinetic evaluation of carbon formation in a membrane reactor for methane reforming. *Chem. Eng. J.* 134 (1–3), 138–144. doi:10.1016/j.cej.2007.03.051

Research and Markets (2019). IPCC Global warning of 1.5°C, summary for policy makers. *Renew. Energy* 2019 (3), 2.

Rice, S. F., and Delmotte, D. M. (2007). *Autothermal reforming of natural gas to synthesis gas*. Reference: KBR Paper #2031. Sand2007-2331. Livermore, California, USA: Sandia National Laboratories.

Rostrup-nielsen, J. R., and Rostrup-nielsen, T. (2002). Large-scale hydrogen production. *CATTECH* 6, 150–159. doi:10.1023/a:1020163012266

Rydén, M., Lyngfelt, A., and Mattisson, T. (2006). Synthesis gas generation by chemical-looping reforming in a continuously operating laboratory reactor. *Fuel* 85 (12–13), 1631–1641. doi:10.1016/j.fuel.2006.02.004

Sasaki, K., Adachi, S., Haga, K., Uchikawa, M., Yamamoto, J., Iyoshi, A., et al. (2019). Fuel impurity tolerance of solid oxide fuel cells. *ECS Trans.* 7 (1), 1675–1683. doi:10.1149/1.2729277

Seemann, M., and Thunman, H. (2019). "Substitute natural gas for waste," in *Ch 9; methane synthesis* (Amsterdam, Netherlands: Elsevier Inc.).

Shi, W., Yang, H., Shen, Y., Fu, Q., Zhang, D., and Fu, B. (2018). Two-stage PSA/VSA to produce H2 with CO2 capture via steam methane reforming (SMR). *Int. J. Hydrogen Energy* 43 (41), 19057–19074. doi:10.1016/j.ijhydene.2018.08.077

Shokrollahi Yancheshmeh, M., Radfarnia, H. R., and Iliuta, M. C. (2016). High temperature CO2 sorbents and their application for hydrogen production by sorption enhanced steam reforming process. *Chem. Eng. J.* 283, 420–444. doi:10.1016/j.cej.2015.06.060

Spallina, V., Pandolfo, D., Battistella, A., Romano, M. C., Van Sint Annaland, M., and Gallucci, F. (2016). Techno-economic assessment of membrane assisted fluidized bed reactors for pure H2 production with CO2 capture. *Energy Convers. Manag.* 120, 257–273. doi:10.1016/j.enconman.2016.04.073

Sub Kwak, B., Park, N. K., Ryu, H. J., Baek, J. I., and Kang, M. (2018). Reduction and oxidation performance evaluation of manganese-based iron, cobalt, nickel, and copper bimetallic oxide oxygen carriers for chemical-looping combustion. *Appl. Therm. Eng.* 128, 1273–1281. doi:10.1016/j.applthermaleng.2017.09.111

Tang, M., Xu, L., and Fan, M. (2015). Progress in oxygen carrier development of methane-based chemical-looping reforming: a review. *Appl. Energy* 151, 143–156. doi:10.1016/j.apenergy.2015.04.017

Tawfik, H., El-Kathib, K., Hung, Y., and Mahajan, D. (2007). Effects of bipolar plate material and impurities in reactant gases on PEM fuel cell performance. *Ind. Eng. Chem. Res.* 46, 8898–8905. doi:10.1021/ie071241j

Turton, R., Bailie, R. C., Whiting, W. B., Shaeiwitz, J. A., and Bhattacharyya, D. (2001). *Analysis, synthesis, and design of chemical processes* London, United Kingdom: Pearson Education.

Xu, G., Liang, F., Yang, Y., Hu, Y., Zhang, K., and Liu, W. (2014). An improved CO2 separation and purification system based on cryogenic separation and distillation theory. *Energies* 7 (5), 3484–3502. doi:10.3390/en7053484

Yan, Y., Manovic, V., Anthony, E. J., and Clough, P. T. (2020). Techno-economic analysis of low-carbon hydrogen production by sorption enhanced steam methane reforming (SE-SMR) processes. *Energy Convers. Manag.* 226, 113530. doi:10.1016/j.enconman.2020.113530

Yukawa, H., Nambu, T., and Matsumoto, Y. (2014). *Design of group 5 metal-based alloy membranes with high hydrogen permeability and strong resistance to hydrogen embrittlement*. Sawston, United Kingdom: Woodhead Publishing Limited.

10.3389/fceng.2024.1294752

Glossary

AR	Air reactor
CaC	Calcium oxide carbonation
CaH	Calcium oxide hydration
CAPEX	Capital Expenditure
CCR	Carbon capture rate
CCS	Carbon capture and sequestration
CCU	Carbon capture and utilization
CLR	Chemical looping reforming
DFBR	Dual fluidized bed reactor
FR	Fuel reactor
HC	Hydrogen combustion
H&MB	Heat and mass balance
H_2O/CH_4	Steam-to-methane molar ratio
HRF	Hydrogen recovery factor
LHV	Low heating value
MA-	Membrane assisted
MC	Methane combustion
MD	Methane decomposition
NG	Natural gas
MC	Methane combustion
O_2/CH_4	Oxygen-to-methane ratio
OPEX	Operational Expenditure
OXOC	Oxidation oxygen carrier
PSA	Pressure swing adsorption
rB	Reverse Boudouard
REDOC	Reduction oxygen carrier
REF	Reformer reactor
REG	Regenerator reactor
SER	Sorption enhanced reforming
SMR	Steam methane reforming
SR	Steam reforming
TFM	Two fluid model

List of symbols

CCR	Carbon capture rate (–)
E	Emission per energy unit (kg/GJ)
f	fraction (–)
F	Molar flow (mol/s)
ΔH_c^0	Enthalpy of combustion (kJ/kg)
ΔH_r^0	Enthalpy of reaction (kJ/mol)
HRF	Hydrogen recovery factor (–)
p	Pressure (bar)
Q_{th}	Thermal energy (J/s)
T	Temperature (K)
W_{el}	Electrical power (J/s)
y	Molar fraction (–)
Y_{H2}	Hydrogen yield (–)
η	Efficiency (–)

Superscript

0	inlet
exp	export
ev	equivalent
imp	import
prd	product
perm	Permeate
ret	retentate
imp	import

Subscript

c	combustion
el	electricity
eq	equilibrium
gg	gas-gas
gl	gas-liquid
hydr	hydraulic
iso	isotropic
mech	mechanical
perm	permeate
pre	pre-reformer
R	Reactor
ret	retentate
th	thermal